Theory of phase-separation dynamics in quenched binary mixtures

Michio Tokuyama

Statistical Physics Division, Tohwa Institute for Science, Tohwa University, Fukuoka 815, Japan

Yoshihisa Enomoto*

Department of Physics, Faculty of Science, Nagoya University, Nagoya 464, Japan
(Received 10 June 1992)

A systematic theory of the dynamics of phase separation of quenched binary systems into metastable states is presented. Not only the kinetic equation for the single-droplet-size distribution function $f(R,t)$ but also the linear equation for the structure function $S(k,t)$, which are valid over the entire time region after the nucleation stage, are derived from a unified point of view. The functions $f(R,t)$ and $S(k,t)$ are shown to satisfy the dynamical scaling relations $f(R,t)=[n(t)/\langle R \rangle (t)]F(R/\langle R \rangle,t)$ and $S(k,t)=[k_M(t)]^{-d}[\Phi(t)]^{\delta}\Psi(k/k_M,t)$ with $k_M^{-1}(t)\propto \langle R \rangle /\Phi^{1/d}$, where n is the number density of the minority phase, $\langle R \rangle$ the average droplet radius, Φ the volume fraction of the minority phase, k_M the peak position of $S(k,t)$, and $d=3$ here. Three characteristic stages are then shown to exist after the nucleation stage: the growth stage with $\delta=2$, where the power laws are given by $\langle R \rangle \propto t^{1/2}$, $n \propto t^0$, $k_M \propto t^0$, and $\Phi \propto t^{3/2}$; the intermediate stage with $\delta=1/d$, where $\langle R \rangle \propto t^{1/4}$, $n \propto t^{-2/3}$, $k_M \propto t^{-2/9}$, and $\Phi \propto t^{1/12}$; and the coarsening stage with $\delta=1/d$, where $\langle R \rangle \propto t^{1/3}$, $n \propto t^{-1}$, $k_M \propto t^{-1/3}$, and $\Phi \propto t^0$. Two crossovers are then observed in the time exponents. The time evolution of the scaling functions $F(\rho,t)$ and $\Psi(x,t)$ are thus studied explicitly, including their asymptotic behavior and their dependence on Φ.

PACS number(s): 64.70.$-$p, 64.60.My, 64.60.Qb

I. INTRODUCTION

Many experimental [1–7], numerical [8–10], and theoretical [11–14] approaches have been applied to study the dynamics of phase separation of the quenched binary systems in the metastable state. When the system is quenched into two phase regions near the coexistence curve from the one-phase region, it undergoes phase separation by nucleation and growth of droplets of the minority phase. The early stage of phase separation has been studied in particular by Becker and Döring [15]. Their theory was then developed into the microscopic cluster theory of nucleation by Binder and Stauffer [16]. The late stage of phase separation was explored in the monumental works by Lifshitz and Slyozov [17] and independently by Wagner [18] (LSW). Since the LSW theory was only available in the limit of zero supersaturation, several attempts [19–21] were recently made to extend it to the case of finite supersaturation. In contrast to the study of the late stage of phase separation, however, the dynamical aspects of the intermediate stage before the late stage are not yet well understood theoretically, although this stage is important for real systems [1–7].

To obtain an understanding of the qualitative features of the dynamical properties of the metastable state, two kinds of experimental methods have been used in the study of first-order phase transitions [22]. One is direct microscope observations. The other is small-angle-scattering measurements. In order to study the dynamics of phase separation, therefore, there are two theoretical aspects, corresponding to those experiments. The first is to study the causal motion of droplet growth, which is observable by an electron microscope [23]. This is de-

scribed by the single-droplet-size distribution function $f(R,t)$ with radius R. Hence the main aim here is to find a kinetic equation for $f(R,t)$ from first principles. The second is to explore the fluctuations around the causal motion. In most cases the fluctuations are small as compared to the causal motion. However, they are still important since they are observable as the structure function $S(k,t)$ by small-angle-scattering experiments [22]. The main theoretical interest here is to find an equation of motion for $S(k,t)$ from a new point of view. In order to obtain such equations from a microscopic point of view, the diffusive long-range interactions among droplets must be studied consistently as a many-body problem. Thus the principal purpose of the present paper is to develop a method of finding not only the kinetic equation for $f(R,t)$ but also the linear equation for $S(k,t)$, which are valid over the entire time region after the nucleation stage, from a unifying point of view, and thereby to formulate a general scheme for understanding the dynamics of phase separation in quenched binary systems from first principles.

We consider a three-dimensional system with volume V, which consists of spherical droplets of the minority phase and a supersaturated solution of the majority phase. There are several mechanisms for growth of droplets, such as an evaporation-condensation mechanism [17] and elastic interactions [24]. In this paper we restrict our attention to the case where diffusion is the only significant transport process and hence the driving force for the coarsening is provided only by the interfacial surface energy. We also restrict ourselves to the case of instantaneous nucleation where all droplets are nucleated only during the initial short time, that is, the nucleation

stage. We further assume that the droplets are nonoverlapping and nontouching spheres and the distribution of their positions is stationary.

The present system has three kinds of time-dependent characteristic lengths and times. The first is an average droplet radius $\langle R \rangle(t)$ and its related microscopic time $t_0(t) = 3\langle R \rangle^2/D$, where D is a diffusion coefficient. The second is an interdroplet distance $L(t)$ and its related time $T_I(t)$,

$$L(t) = [4\pi n(t)/3]^{-1/3}, \quad T_I(t) = 3L^2/D , \quad (1.1)$$

where $n(t)$ denotes the number of droplets per unit volume. The third is a screening length $l(t)$ over which the diffusive interactions are screened out, and a screening time $T(t)$,

$$l(t) = [4\pi n(t)\langle R \rangle(t)]^{-1/2}, \quad T(t) = 3l^2/D . \quad (1.2)$$

Let $\Phi(t) = 4\pi n(t)\langle R^3 \rangle(t)/3$ and $\Delta(t)$ denote the volume fraction of droplets and the supersaturation at time t, respectively, where the brackets denote the average over the distribution $f(R,t)$. Since the total mass of droplets is conserved, we then have

$$\Phi(t) + \Delta(t) = Q , \quad (1.3)$$

where Q represents the total supersaturation. In this paper we discuss only the cases where Q is small but finite. Hence we obtain

$$\langle R \rangle/L \sim \Phi^{1/3}, \quad L/l \sim \Phi^{1/6}, \quad \langle R \rangle/l \sim \Phi^{1/2} . \quad (1.4)$$

This leads to the inequalities

$$\langle R \rangle \ll L \ll l, \quad t_0 \ll T_I \ll T . \quad (1.5)$$

Thus the volume fraction Φ turns out to be a small parameter in the present system.

After the nucleation stage, there are two kinds of growth mechansims which cause droplet growth. The first is a direct growth mechanism where the droplets grow directly from the supersaturated solution by diffusion. This mechanism does not change the number of droplets. The second is the Ostwald ripening (or coarsening) mechanism, where the larger droplets grow at the expense of the smaller ones which disappear. This mechanism reduces the number of droplets in such a way that the volume fraction does not change. These mechanisms become important on different time scales. In order to describe this, therefore, it is convenient to introduce the following three time-independent macroscopic times. The first is an initial time of growth, $T_0 = R_0^2/DQ$, at which the growth from the solution starts, where R_0 is the initial critical radius. The second is a screening time, $T_s = 3/[4\pi n(0)R_0 D]$, over which the screening interaction between droplets becomes important. The third is a coarsening time T_c over which the growth from the solution is over and the Ostwald ripening mechanism dominates the system. Here $t_0 \ll T_0 \ll T_s \ll T_c$. On the time scale of order T_0, the direct growth mechanism dominates the system. Since the many-body effect is not important, the rapid growth from the solution proceeds independently. On the time scale of order T_s, however,

the droplets separated by a distance of order l start to interact through diffusion. Hence two kinds of growth mechanisms compete with each other through the diffusive long-range interaction. Thus, the growth is no longer independent and is slowed down by such a long-range interaction. On the time scale of order T_c, only the coarsening mechanism dominates the system.

In Sec. III we derive the Fokker-Planck type kinetic equation for the distribution function $f(R,t)$ up to order $\Phi^{1/2}$. In Sec. IV we also derive the linear non-Markov equation with the source term for the dynamical structure function $S(k,t)$. Both equations are valid on the entire time region after the nucleation stage. Since they do not contain any adjustable parameters, the time evolution of $f(R,t)$ and $S(k,t)$ are obtained by just solving them under appropriate boundary and initial conditions. The central results are as follows. The distribution function $f(R,t)$ is shown to satisfy scaling

$$f(R,t) = [n(t)/\langle R \rangle(t)]F(R/\langle R \rangle,t) , \quad (1.6)$$

with the coarsening rate

$$K(t) = \lim_{\rho \to 0} F(\rho,t)/\rho^2 , \quad (1.7)$$

where $F(\rho,t)$ denotes the relative-droplet-size distribution function. The dynamical structure function $S(k,t)$ is also shown to satisfy a new scaling form

$$S(k,t) = k_M^{-d}\Phi^{\delta}\Psi(k/k_M,t) , \quad (1.8)$$

with the peak position of $S(k,t)$ as a function of k,

$$k_M^{-1}(t) = c_2\langle R \rangle/\Phi^{1/d} = (c_2/\mu_3^{1/3})L(t) , \quad (1.9)$$

where c_2 is a positive constant, $\mu_3(t) = \langle R^3 \rangle/\langle R \rangle^3$, and $d = 3$ here. The value of the exponent δ depends on the time region. The scaling function $\Psi(x,t)$ has the asymptotic form

$$\Psi(x,t) \sim \begin{cases} x^4 & \text{for } x \ll 1 \\ x^{-4} & \text{for } x \gg 1 , \end{cases} \quad (1.10)$$

where $x = k/k_M$. The x^4 dependence of $\Psi(x)$ for small x is caused by the nonthermal fluctuations generated by the long-range interactions among droplets. This behavior agrees with recent theories [25–28]. The x^{-4} tail of $\Psi(x)$ for large x, known as Porod's law, results from the fact that the droplets are assumed to have a sharp interface after the nucleation stage.

Three characteristic stages are shown to exist after the nucleation stage. The first is a growth stage $[G]$ where $T_0 \leq t < T_s$, and $\delta = 2$. The interactions among droplets are not important, and the droplets, which have reached an appreciable size, that is, the initial critical radius R_0, grow directly and independently from the solution. The distribution function $F(\rho,t)$ is given by

$$F(\rho,t) = \delta(\rho - 1) . \quad (1.11)$$

Then, the temporal power laws are given by

$$\langle R \rangle(t) \sim t^{1/2}, \quad n(t) = n(0), \quad \Phi(t) \sim t^{3/2} ,$$
$$K(t) = 0, \quad k_M(t)^{-1} \sim t^0, \quad S_M(t) \sim t^3 , \quad (1.12)$$

where $S_M = S(k_M, t)$ denotes the peak height of $S(k,t)$. The number density $n(t)$ remains constant and the volume fraction $\Phi(t)$ increases rapidly. The power-law behavior is in good agreement with the recent experiments of Cumming et al. [7]. After this stage, two kinds of growth mechanisms compete with each other through the diffusive long-range interactions. This is an intermediate stage $[I]$, where $T_s \leq t < T_c = T_s [n(0)/K(\infty)\mu_3(\infty)n(T_s)]^3$, and $\delta = 1/d$. The distribution function $F(\rho, t)$ can be obtained only numerically here. The temporal power laws are then given by

$$\langle R \rangle(t) \sim t^{1/4}, \quad n(t) \sim t^{-2/3}, \quad \Phi(t) \sim t^{1/12},$$
$$K(t) \sim t^{-1/4}, \quad k_M(t)^{-1} \sim t^{2/9}, \quad S_M(t) \sim t^{25/36}.$$
(1.13)

The growth is thus slowed down by the long-range interactions.

The last is a coarsening stage $[C]$ where $T_c \leq t$, and $\delta = 1/d$. The growth is governed only by the Ostwald ripening mechanism. This stage further consists of two time regions. One is a transient stage with the time region $T_c \leq t \ll T_L$, where the volume fraction Φ is increasing slowly in time as

$$\Phi(t) = Q\{1 - [K(\infty)t/T_0]^{-1/3}\}.$$
(1.14)

Here $T_L = 0.02^{-3}[T_0/K(\infty)]$ represents the late stage time over which the deviation of Φ from Q becomes less than 2%. Hence the scaling functions $F(\rho, t)$ and $\Psi(x, t)$ still depend on time through $\Phi(t)$. The temporal power laws are then given by

$$\langle R \rangle(t) \sim t^{1/3}[1 + A_1 t^{-1/3}]^{1/3},$$
$$n(t) \sim t^{-1}[1 - A_2 t^{-1/3}],$$
$$K(t) \sim K(\infty)[1 + A_3 t^{-1/3}],$$
$$k_M(t)^{-1} \sim \langle R \rangle / \Phi^{1/3}, \quad S_M(t) \sim k_M^{-3} \Phi^{1/3},$$
(1.15)

where A_i are positive constants. The other is a late stage with $T_L < t$, where $\Phi = Q$. The scaling functions $F(\rho, t)$ and $\Psi(x, t)$ become independent of time. The temporal power laws are then given by

$$\langle R \rangle(t) \sim t^{1/3}, \quad n(t) \sim t^{-1}, \quad \Phi(t) = Q,$$
$$K(t) = K(\infty), \quad k_M(t)^{-1} \sim t^{1/3}, \quad S_M(t) \sim t.$$
(1.16)

The temporal power behavior of the late stage agrees with those expected on the basis of the LSW theory, while the quantitative behavior of $F(\rho, t = \infty)$ and $\Psi(x, t = \infty)$ agrees with those obtained previously by Tokuyama, Tawasaki, and Enomoto [19], referred to as TKE.

The dynamical scalings, Eqs. (1.6) and (1.8), hold over the entire time region after the nucleation stage. Thus, in stage $[I]$, the two lengths $\langle R \rangle$ and L are relevant, while only one length $\langle R \rangle$ is relevant in stages $[G]$ and $[C]$. The two crossovers are then observed in the time exponents of $\langle R \rangle$ and n around T_s and T_c. These qualitative changes are caused by the static long-range interaction among droplets (screening interaction) of order Φ^0,

which becomes important on the time scale of order T. The first crossover is attributed to a transition from the single-body type to the many-body type growth from the solution, while the second one corresponds to a transition from the many-body type growth to the coarsening process. There is also a dynamic long-range interaction (spatial correlation) of order $\Phi^{1/2}$, which becomes important on the time scale of order $T/\Phi^{1/2}$. This alters only the quantitative behavior of $f(R, t)$ and $S(k, t)$, leading to their dependence on Q.

The outline of this paper is as follows. In Sec. II we first derive the basic equations for the radius of each droplet from the diffusion equation. In Sec. III we then transform them into the hierarchy equations for the multibody distribution functions. By employing the systematic expansion method in powers of $\Phi^{1/2}$, we truncate them to obtain the kinetic equation for the single-droplet-size distribution function $f(R, t)$ and the linear variance equation for the fluctuations, to order $\Phi^{1/2}$. This is all done by employing a similar formalism to that previously introduced by one of the present authors (M.T) [29] to study the kinetics of electrochemical nucleation on a substrate. The time evolution of $f(R, t)$, its scaling behavior, and its volume fraction dependence are then discussed. In Sec. IV we further derive the non-Markov linear equation with the source term for the structure function $S(k, t)$ from the variance equation. The time evolution of $S(k, t)$ is thus explicitly explored, including its scaling behavior, and its volume fraction dependence. Section V is devoted to conclusions.

II. BASIC EQUATIONS

Here we describe a derivation of a model equation to study a diffusion-controlled growth of spherical droplets.

The molar concentration field of the supersaturated solution is described by the diffusion equation

$$\frac{\partial}{\partial t} C(\mathbf{r}, t) = D \nabla^2 C(\mathbf{r}, t),$$
(2.1)

with the full initial and boundary conditions

$$C(\mathbf{r}, t = 0) = C(|\mathbf{r}| = \infty, t) = C_b,$$
(2.2)

$$C(\mathbf{r} = \mathbf{x}_i, t) = C_\infty + \rho_m \alpha / R_i,$$
(2.3)

where D is the diffusion coefficient of the solute, C_b the bulk concentration field, C_∞ the equilibrium solubility of a droplet of infinite radius, ρ_m the molar density of the material composing the droplet, α the capillary length, and R_i the radius of the droplet i. Here $\mathbf{x}_i = \mathbf{X}_i + \mathbf{R}_i(t)$ denotes the position vector from the origin to a point on the surface of the ith droplet, where $\mathbf{X}_i = (X_i, Y_i, Z_i)$ is the position vector from the origin to the center of the ith droplet, and $\mathbf{R}_i(t)$ is the radius vector from the center of the ith droplet to a point on its surface.

We now derive an equation of motion for the radius of the ith droplet, $R_i(t)$. Since the conservation of mass holds for each droplet, the time evolution of the mass of the ith droplet is described by

$$\rho_m \frac{d}{dt}\left[\frac{4\pi R_i(t)^3}{3}\right] = DR_i^2 \int_{S_i} d\Omega_i (\mathbf{e}_i \cdot \mathbf{\nabla} C)|_{\mathbf{r}=\mathbf{x}_i} , \qquad (2.4)$$

where Ω_i denotes the orientation of the vector $\mathbf{R}_i$, $\mathbf{e}_i$ the unit normal vector to the interface of the ith droplet from inside to outside, and S_i the surface of the ith droplet over which the integral is taken. By adding an appropriate source term to Eq. (2.1), the boundary conditions (2.2) and (2.3) can be eliminated from Eq. (2.1). As is shown in Appendix A, by solving such a diffusion equation and inserting its formal solution into Eq. (2.4), we thus obtain, on the length scale of order l,

$$\frac{d}{dt}R_i(t) = \frac{\alpha D}{R_i(t)^2} M_i(t) , \qquad (2.5)$$

with the source-sink strength

$$M_i(t) = \frac{R_i(t)}{R_0} - 1$$
$$-4\pi DR_i \sum_{j(\neq i)}^{N} \int_0^t ds \frac{\exp[-|\mathbf{X}_{ij}|^2/4Ds]}{(4\pi Ds)^{3/2}}$$
$$\times M_j(t-s) , \qquad (2.6)$$

where $R_0 = \alpha/Q$ is the initial critical radius, $Q = (C_b - C_\infty)/\rho_\infty$ being the total supersaturation, and $\mathbf{X}_{ij} = \mathbf{X}_i - \mathbf{X}_j$. Equation (2.5) is a new starting equation to study the kinetics of phase separation over the entire time region after the nucleation stage. It is a non-Markov equation and is different from the Markov equation previously obtained by several authors [21,30–32] to study the late stage of coarsening. If one makes a Markov approximation in Eq. (2.6), however, Eq. (2.5) exactly reduces to the same Markov equation as that obtained previously.

Equation (2.5) represents a mass conservation for each droplet. Since the total mass is also conserved, it must be supplemented by another conservation law. Hence let us define a homogeneous supersaturation by

$$\Delta(t) = \frac{1}{n(t)V} \sum_{i=1}^{N} \overline{\Delta_i(t)} , \qquad (2.7)$$

where the bar denotes the average over a suitable initial statistical ensemble, and V the total volume of the system. Here $n(t)$ represents the number density of droplets,

$$n(t) = V^{-1} \int d\mathbf{r} \int dR \, f(R,\mathbf{r};t) , \qquad (2.8)$$

with the single-droplet distribution function with radius R and at the position $\mathbf{r}$,

$$f(R,\mathbf{r};t) = \overline{N(R,\mathbf{r};t)} , \qquad (2.9)$$

where $N(R,\mathbf{r};t)$ denotes the droplet number density defined by

$$N(R,\mathbf{r};t) = \sum_{i=1}^{N} \delta(R - R_i(t))\delta(\mathbf{r} - \mathbf{X}_i(0)) . \qquad (2.10)$$

Using Eqs. (2.5) and (2.7), we thus find the conservation of mass for the entire system,

$$\Phi(t) + \Delta(t) = \Phi_0 + \Delta_0 = Q , \qquad (2.11)$$

with the volume fraction of the droplets,

$$\Phi(t) = \frac{1}{V} \int d\mathbf{r} \int dR \frac{4\pi R^3}{3} f(R,\mathbf{r};t) , \qquad (2.12)$$

where $\Phi_0 = \Phi(0)$ and $\Delta_0 = \Delta(0)$.

The second term of Eq. (2.6) represents the many-body effect due to the spatial long-range interactions among droplets separated by a distance of order l and contains the higher-order terms in $\Phi^{1/2}$. Because of such long-range interactions, it is beyond our capacity to deal with Eq. (2.5) analytically, although it is possible to solve it numerically by computer simulations. Hence we must further reduce it to obtain macroscopic equations, which we can reasonably analyze. As discussed in Sec. I, there are two theoretical aspects, depending on what processes we are interested in. The first is to study the causal motion of growth which is described by the single-droplet-size distribution function $f(R,\mathbf{r};t)$. The second is to explore the fluctuations $\delta N(R,\mathbf{r};t)$ around the causal motion $f(R,\mathbf{r};t)$, where $\delta N(R,\mathbf{r};t) = N(R,\mathbf{r};t) - f(R,\mathbf{r};t)$. In most cases, they are small as compared to the causal motion. However, they are important since they are experimentally observable through the structure function $S(k,t)$ by using small-angle scattering of neutrons, x rays, or light [21,32]. As is discussed in Sec. III, it is also indispensable to explore the dynamics of the fluctuations explicitly since the derivation and validity of the kinetic equation for $f(R,\mathbf{r};t)$ is closely related to their asymptotic behavior. The fluctuations are customarily described by the variance,

$$\chi(R_1,\mathbf{r}_1,R_2,\mathbf{r}_2;t) = \overline{\delta N(R_1,\mathbf{r}_1;t)\delta N(R_2,\mathbf{r}_2;t)} . \qquad (2.13)$$

The spherically averaged structure function $S(k,t)$ is then simply related to the fluctuations δN through the variance χ by

$$S(k,t) = R_0^{-3} \int_0^\infty dR_1 \int_0^\infty dR_2 \frac{4\pi R_1^3}{3} \frac{4\pi R_2^3}{3}$$
$$\times \psi(kR_1)\psi(kR_2)\chi_k(R_1,R_2;t) , \qquad (2.14)$$

with a structure factor of a single droplet,

$$\psi(x) = 3(\sin x - x \cos x)/x^3 , \qquad (2.15)$$

where $k = |k|$, and χ_k is defined by

$$\chi_k(R_1,R_2;t) = R_0^{-5} \int d\mathbf{r}_{12} \exp[-i\mathbf{k}\cdot\mathbf{r}_{12}]\chi(1,2;t) . \qquad (2.16)$$

In order to study the dynamics of phase separation, therefore, we need to discuss both the time evolution of the single-droplet-size distribution function f and that of the variance χ. In the next sections we derive the kinetic equations for them from Eq. (2.5) by employing a systematic expansion method in powers of $\Phi^{1/2}$.

III. KINETIC EQUATIONS

In the present section, we derive the kinetic equation for the single-droplet-size distribution function for $f(R,r;t)$ from Eq. (2.5), up to order $\Phi^{1/2}$ and discuss its asymptotic behavior.

A. Hierarchy equations for distribution functions

Define the probability distribution function of m droplets by

$$f_m(1,\ldots,m;t)=\prod_{\substack{i,j \\ (i\neq j)}}^{m}\Theta(|\mathbf{r}_{ij}|-R_i-R_j)$$
$$\times \overline{N(1;t)\cdots N(m;t)}\ ,\qquad (3.1)$$

where $i=(R_i,\mathbf{r}_i)$ represents the specific value of the radius and position of the ith droplet. Here the step function $\Theta(x)$ of Eq. (3.1), $\Theta(x)=1$ for $x>0$ and $\Theta(x)=0$ for $x\leq 0$, comes from the fact that the droplets are supposed to be nonoverlapping and nontouching. The average radius $\langle R\rangle(t)$ is now defined by

$$\langle R\rangle(t)=\int d(1)R_1f_1(1;t)/n(t)V\ ,\qquad (3.2)$$

where $d(i)=dR_id\mathbf{r}_i$.

The droplet number density $N(i;t)$ can be split up into a deterministic part $f_1(i;t)$ and a fluctuating part $\delta N(i;t)$,

$$N(i;t)=f_1(i;t)+\delta N(i;t)\ .\qquad (3.3)$$

This decomposition is essential since the Φ dependence of the fluctuations differs from that of the deterministic part. In fact, we show below that the relative magnitude of the fluctuations compared to the deterministic part is of order $\Phi^{(d-2)/4}$, where $d=3$ here. Hence it is convenient further to introduce the correlation functions $G_m(1,\ldots,m;t)$ through the Ursell-Mayer procedure,

$$f_2(1,2)=f(1)f(2)+G_2(1,2)\ ,$$

$$f_3(1,2,3)=f(1)f(2)f(3)+(1+e_{12}+e_{13})f(1)G_2(2,3)$$
$$+G_3(1,2,3)\ ,\qquad (3.4)$$

and so on, where $f(i)=f_1(i;t)$, and e_{ij} is the exchange operator between i and j.

By taking the time derivative of Eq. (3.1) and then using Eq. (2.5), we thus obtain

$$\frac{\partial}{\partial t}f_m(1,\ldots,m;t)=\alpha D\sum_{i=1}^{m}e_{mi}\frac{\partial}{\partial R_m}\frac{1}{R_m^2}I_m(1,\ldots,m)\ ,$$
$$(3.5)$$

with

$$I_m(1,\ldots,m;t)=\prod_{\substack{i,j \\ (i\neq j)}}^{m}\Theta(|\mathbf{r}_{ij}|-R_i-R_j)$$
$$\times \overline{N(1)\cdots N(m)k(m;t)}\ ,\qquad (3.6)$$

where

$$k(i;t)=1-\frac{R_i}{R_0}\left[1+4\pi DR_0\int_0^t ds\int d(j)g_{ij}^0(t-s)\Theta(|\mathbf{r}_{ij}|-R_i-R_j)N(j;s)k(j;s)\right]\ .\qquad (3.7)$$

Here the free propagator g_{ij}^0 is defined by

$$g_{ij}^0(t)=\exp[-|\mathbf{r}_{ij}|^2/4Dt]/(4\pi Dt)^{3/2}\ .\qquad (3.8)$$

By using Eqs. (3.1) and (3.4), we also obtain

$$\frac{\partial}{\partial t}G_m(1,\ldots,m;t)=\alpha D\sum_{i=1}^{m}e_{mi}\frac{\partial}{\partial R_m}\frac{1}{R_m^2}J_m(1,\ldots,m)\ ,$$
$$(3.9)$$

with

$$J_1(1)=I_1(1)\ ,$$

$$J_2(1,2)=I_2(2,1)-I_1(2)f(1)\ ,$$

$$J_3(1,2,3)=I_3(3,2,1)-I_2(3,2)f(1)-I_2(3,1)f(2)$$
$$-I_1(3)G_2(2,1)+I_1(3)f(2)f(1)\ ,\qquad (3.10)$$

and so on. Use of Eqs. (2.13), (3.1), (3.3), and (3.4) then leads to

$$\chi(1,2;t)=\delta(1-2)f(1)+G_2(1,2)\ .\qquad (3.11)$$

By taking the time derivative of Eq. (3.11) and using Eqs. (3.5) and (3.9), we obtain

$$\frac{\partial}{\partial t}\chi(1,2;t)=\alpha D(1+e_{12})\frac{\partial}{\partial R_2}\frac{1}{R_2^2}[\ \delta(1-2)J_1(2)$$
$$+J_2(2,1)]\ .\qquad (3.12)$$

Equations (3.5), (3.9), and (3.12) give the system of kinetic equations which describes not only the deterministic motion of growth, but also the fluctuations around it at the microscopic level. Those equations are written in terms of J_m. Since J_m is in general a functional of the distribution function f_m ($n\leq m$), however, they become hierarchy equations. Hence we next introduce the systematic expansion method in $\Phi^{1/2}$ and then extract the macroscopic kinetic equations from such hierarchy equations by exploring the asymptotic forms of J_m.

B. Systematic expansion method in $\Phi^{1/2}$

Here we introduce the systematic expansion method [28,33] which can be used to extract the kinetic process characterized by the length and time scale (l,T) from the microscopic process described by $(\langle R\rangle,t_0)$ systematically. Since $l\gg\langle R\rangle$ and $T\gg t_0$, we introduce a scale transformation,

$$l \rightarrow Sl, \quad T \rightarrow S^{\phi}T \; , \tag{3.13}$$

with $S \gg 1$, where $\langle R \rangle$, t_0, and all microscopic quantities such as D and ρ_m are fixed. Use of Eqs. (1.2), (1.3), and (3.13) leads to

$$n \rightarrow S^{-2}n, \quad \Phi \rightarrow S^{-2}\Phi, \quad \Delta \rightarrow S^{-2}\Delta \; , \tag{3.14}$$

$$Q \rightarrow S^{-2}Q, \quad \alpha \rightarrow S^{-2}\alpha \; ,$$

where R_0 is fixed. Since $T = 3l^2/D$, the time exponent ϕ is given by $\phi = 2$. The space-time coarse graining is then given by

$$r \rightarrow Sr, \quad t \rightarrow S^2 t \; , \tag{3.15}$$

for distances $|r|$ of order l and time intervals t of order T. Hence we find the thermodynamic limit,

$$N \rightarrow S^{d-2}N, \quad V \rightarrow S^d V \; . \tag{3.16}$$

Use of Eqs. (2.8) and (3.14)–(3.16) thus leads to the scaled form

$$f(R,\mathbf{r};t) = \frac{n(t)}{\langle R \rangle(t)} \tilde{f} \left[\frac{R}{\langle R \rangle}, \frac{\mathbf{r}}{l}; \frac{t}{T} \right] \; , \tag{3.17}$$

where $\tilde{f}$ is a scale invariant.

Since the Φ dependence of the fluctuations δN will differ from that of the deterministic motion $f(R,r;t)$, we define a scaling exponent κ by

$$\delta N(R,\mathbf{r};t) = \left[\frac{3\Phi^{\kappa}}{4\pi \langle R \rangle^{d+5}} \right]^{1/2} \delta \tilde{N} \left[\frac{R}{\langle R \rangle}, \frac{\mathbf{r}}{l}; \frac{t}{T} \right] \; , \tag{3.18}$$

which is combined with Eq. (2.13) to give the scaled form

$$\chi(1,2;t) = \frac{3\Phi^{\kappa}}{4\pi \langle R \rangle^{d+5}} \tilde{\chi} \left[\frac{R_1}{\langle R \rangle}, \frac{R_2}{\langle R \rangle}, \frac{\mathbf{r}_1}{l}, \frac{\mathbf{r}_2}{l}; \frac{t}{T} \right] \; , \tag{3.19}$$

where κ is an exponent to be determined and represents the magnitude of χ. Thus the systematic expansion method not only permits us to carry out the space-time coarse graining in a manner consistent with the expansion in $\Phi^{1/2}$ but also enables us to evaluate the magnitude of the fluctuations relative to the deterministic motion, $|\delta N/f| \sim \Phi^{(\kappa-2)/2}$.

We next discuss the correlation functions G_m. There are two types of correlation functions which originate from different interactions. One is the spatial correlation due to the short-range interactions over a distance of order $\langle R \rangle$. As is easily shown, this gives a higher-order contribution in $\Phi^{1/2}$. The other correlation is due to the long-range interactions over a distance of order l. This has the invariant form

$$G_m(1, \ldots, m; t)$$

$$\sim \Phi^{\kappa_m} \tilde{G}_m \left[\frac{R_1}{\langle R \rangle}, \ldots, \frac{R_m}{\langle R \rangle}, \frac{\mathbf{r}_1}{l}, \ldots, \frac{\mathbf{r}_m}{l}; \frac{t}{T} \right] \; , \tag{3.20}$$

where κ_m is a scaling exponent to be determined. We should note here that in the present system an interaction between two touching droplets such as a coagulation does not occur since the centers of droplets are assumed to be fixed and to be separated by a distance of order l.

The scaling exponent κ_m can be obtained by integrating f_m and G_m with respect to $r_1 \ldots r_m$ over the volume l^d. Since $f_m \sim n^m$, we have $\int d(1) \ldots \int d(m) f_m \sim (nl^d)^m$. Since the correlation G_m is nonvanishing only for relative distances shorter than l, we also find $\int d(1) \ldots \int d(m) G_m \sim nl^d$. Then $G_m \sim f_m(nl^d)^{-(m-1)} \sim nl^{-(m-1)d}$. This is combined with Eq. (3.20) to give

$$\kappa_m = 1 + (m-1)d/2, \quad \kappa = \kappa_2 = (d+2)/2 \; . \tag{3.21}$$

By using Eqs. (3.17)–(3.21), we find

$$|\delta N/f|^2 \sim |\chi/f^2| \sim \Phi^{(d-2)/2} \; , \tag{3.22a}$$

$$|G_2/f^2| \sim |G_3/fG_2| \sim \Phi^{(d-2)/2} \; . \tag{3.22b}$$

When $d = 3$, therefore, the relative magnitude of the fluctuations $\delta N(i)$ to the deterministic motion $f(i)$ is small and the higher-order correlations are less important. Hence the hierarchy of Eqs. (3.5) and (3.9) can be truncated. Thus all macroscopic properties are described by the closed equations for the single distribution function f and the variation χ.

We now scale the deterministic equation (3.5). Use of Eqs. (3.13)–(3.17) leads to

$$\frac{\partial}{\partial t} f(R,\mathbf{r};t) = \alpha D \frac{\partial}{\partial R} \frac{1}{R^2} J_1^S(R,S\mathbf{r};S^2 t) \; , \tag{3.23}$$

where the scaled function J_1^S also depends on S through Φ included implicitly in it. Next we scale Eqs. (3.9) and (3.12) for the correlations. Similarly to Eq. (3.23), we obtain

$$\frac{\partial}{\partial t} \chi(1,2;t) = \alpha D (1 + e_{12}) \frac{\partial}{\partial R_2} \frac{1}{R_2^2}$$

$$\times [\delta(1-2) J_1^S(R_2,S\mathbf{r}_2;S^2 t)$$

$$+ S^d J_2^S(R_2,S\mathbf{r}_2,R_1,S\mathbf{r}_1;S^2 t)] \; , \tag{3.24}$$

$$\frac{\partial}{\partial t} G_2(1,2;t) = \alpha D (1 + e_{12}) \frac{\partial}{\partial R_2} \frac{1}{R_2^2}$$

$$\times S^d J_2^S(R_2,S\mathbf{r}_2,R_1,S\mathbf{r}_1;S^2 t) \; , \tag{3.25}$$

and so on. Thus the discussion to find the closed equations for f and χ reduces to the analysis of the scaled functions J_m^S. Hence we next order all terms in J_m^S in the scaling parameter S^{-1}.

C. Kinetic equations up to order $\Phi^{1/2}$

As is shown in Appendix B, expanding the scaled function J_1^S in powers of S^{-1} leads to

$$J_1^S(R_1,S\mathbf{r}_1;S^2 t) = \lambda(1;t)f(1;t)$$

$$+ S^{-1}[v(1;t) + \Lambda(1;t)]f(1;t)$$

$$+ O(S^{-2}) \; , \tag{3.26}$$

with the screening terms,

$$\lambda(1;t)=1-\beta(\mathbf{r}_1;t)\rho_1(t) ,$$

$$v(1;t)=(4\pi D)^2\int_0^t dt_2\int_0^{t_2}dt_3\int d(2)[\ R_1 g_{12}^0(t-t_2,t)R_2 g_{21}(t_2-t_3,t)\lambda(1;t_3)f(2;t_2)$$

$$-4\pi D\int_0^{t_3}dt_4\int d(3)R_1 g_{12}(t-t_2,t)R_2 g_{23}^0(t_2-t_3,t)$$

$$\times R_3 g_{32}(t_3-t_4,t)\lambda(2;t_4)f(2;t)f(3;t_3)] , \tag{3.28}$$

and the correlation term,

$$\Lambda(1;t)=-\frac{4\pi D}{f(1;t)}\int_0^t dt_2\int d(2)R_1 g_{12}(t-t_2,t)m_{21}(t_2,t)G_2(1,2;t) , \tag{3.29}$$

where

$$\beta(\mathbf{r}_1;t)=\langle a\rangle+4\pi D\langle R\rangle\int_0^t ds\int d(2)g_{12}^0(t-s)\lambda(2;s)f(2;s) \tag{3.30a}$$

$$=\langle a\rangle+4\pi D\langle R\rangle\int_0^t ds\int d(2)g_{12}(t-s,t)(1-a_2)f(2;s) . \tag{3.30b}$$

Here the relative droplet size $\rho(t)$ and the reduced droplet radius a are defined by

$$\rho(t)=R/\langle R\rangle(t)=a/\langle a\rangle, \quad a=R/R_0 . \tag{3.31}$$

The screening operator m_{21} is given by

$$m_{21}(t_2,t)=\lambda(2;t_2)-4\pi Df(1;t)\int_0^{t_2}dt_3\int d(3)R_2 g_{23}(t_2-t_3,t)\lambda(3;t_3)e_{31} , \tag{3.32}$$

with the renormalized propagator defined through

$$g_{ij}(s,t)=g_{ij}^0(s)-4\pi D\int_0^s dt_n\int d(n)g_{in}^0(t_n)R_n g_{nj}(s-t_n,t)f(n;t-t_n) , \tag{3.33}$$

where the free propagator g_{ij}^0 is given by Eq. (3.8). In the scaling limit $S\to\infty$, use of Eqs. (3.23) and (3.26) thus leads to

$$\frac{\partial}{\partial t}f(1;t)=\alpha D\frac{\partial}{\partial R_1}\frac{1}{R_1^2}\lambda(1;t)f(1;t) . \tag{3.34}$$

This is the kinetic equation which describes the growth process of droplets with the length scale of order l and the time scale of order T. The screening term $\lambda(1;t)$ is of order Φ^0 and consists of two effects; the single-body effect, which is given by the first term of Eq. (3.30a), and the static many-body (screening) effect due to the long-range interactions among droplets, which is given by the second term of Eq. (3.30a). The screening effect leads to a screening of the free propagator g_{ij}^0, and the diffusive field around a droplet is effectively screened out by the other droplets for distances greater than l [see Eq. (3.48)].

The first-order correction to Eq. (3.34) is given by the second term of Eq. (3.26) and consists of two kinds of many-body effects. One is a static many-body (screening) effect $v(1;t)$, which contains the product of the single distribution functions. The other is a dynamic many-body (correlation) effect $\Lambda(1;t)$, which contains the correlation function G_2. As is shown in Appendix C, the correlation function G_2 obeys the following equation in the scaling limit $S\to\infty$:

$$\frac{\partial}{\partial t}G_2(1,2;t)=\alpha D(1+e_{12})\frac{\partial}{\partial R_2}\frac{1}{R_2^2}$$

$$\times\left[m_{22}(t,t)G_2(1,2;t)\right.$$

$$-\int_0^t dt_3 R_2 g_{21}(t-t_3,t)\lambda(1;t_3)$$

$$\left.\times f(1;t)f(2;t)\right] . \tag{3.35}$$

Hence $G_2(1,2;t)$ is given by the formal solution, to order Φ^0,

$$G_2(1,2;t)=-\alpha D\int_0^t ds\exp\left[\alpha D\int_0^s dx(1+e_{12})\frac{\partial}{\partial R_2}\frac{1}{R_2^2}m_{22}(t-x,t)\right]$$

$$\times(1+e_{12})\frac{\partial}{\partial R_2}\frac{1}{R_2}\int_0^{t-s}dt'g_{21}(t',t)\lambda(1;t-s-t')f(2;t-s)f(1;t-s) , \tag{3.36}$$

where we have neglected the initial correlation $G_2(1,2;t=0)$ since it represents the correlation of the two droplets separated far apart initially before the diffusive interaction.

The correlation term Λ is next dominant since it is of order $\Phi^{1/2}$. If the volume fraction Φ is not sufficiently small, however, it becomes important on a time scale longer than T. In fact, balancing the term $(\partial/\partial t)f(1;t)$ and the next-dominant terms in Eq. (3.23) leads to the time exponent $\phi=3$. Hence there are two time scales. One is the time scale T with $\phi=2$, on which the screening effect is dominant. The other is $T'=T/\Phi^{1/2}$ with $\phi=3$, on which the spatial correlations become important. On the time scale of order T', therefore, the single distribution function $f(1;t)$ consists of a double-time process. By adding the time scale T' we can generalize Eq. (3.17) AS

$$f(R,\mathbf{r};t)=\frac{n(t)}{\langle R\rangle(t)}\tilde{f}\left[\rho,\frac{\mathbf{r}}{l};\frac{t}{T},\frac{t}{T'}\right] .$$ (3.37)

The time derivative of Eq. (3.37) then leads to

$$\frac{\partial}{\partial t}f(1;t)=\frac{1}{T}\left[\frac{\partial}{\partial t'}+\Phi^{1/2}\frac{\partial}{\partial t''}\right]f(1;t',t'') .$$ (3.38)

Here the first term of Eq. (3.38) balances the most-dominant term (λf) in Eq. (3.26), and the second term balances the correction terms $(v+\Lambda)f$ in Eq. (3.26). Thus the double-time scaling $t\to S^2 t$ and $t\to S^3 t$ leads, in the scaling limit $S\to\infty$, to

$$\frac{\partial}{\partial t}f(1;t)=\alpha D\frac{\partial}{\partial R_1}\frac{1}{R_1^2}[\lambda(1;t)+v(1;t)+\Lambda(1;t)]f(1;t) ,$$ (3.39)

with the screening term

$$v(1;t)=m_{11}(t)\int d(2)\rho_1\xi_{12}^0\rho_2\xi_{21}(t)f(2;t) ,$$ (3.40)

and the correlation term

$$\Lambda(1;t)=-\int d(2)\rho_1\xi_{12}(t)m_{21}(t)G_2^\infty(1,2;t)/f(1) ,$$ (3.41)

where the pair correlation function G_2^∞ is given by

$$G_2^\infty(1,2;t)=-\int_0^\infty ds\,\exp\left[s\alpha D(1+e_{12})\left[\frac{\partial}{\partial R_2}\right]R_2^{-2}m_{22}(t)\right]\alpha D(1+e_{12})\left[\frac{\partial}{\partial R_2}\right]R_2^{-1}\xi_{21}(t)\lambda(1;t)f(1;t)f(2;t) .$$ (3.42)

The screening operator m_{21} is given by

$$m_{21}(t)=\lambda(2;t)-f(1;t)\int d(3)\rho_2\xi_{23}(t)\lambda(3;t)e_{31} ,$$ (3.43)

where $\xi_{12}(t)$ is a reduced renormalized propagator given by

$$\xi_{12}(t)=4\pi D\langle R\rangle\int_0^\infty ds\,g_{12}(s,t) .$$ (3.44)

The reduced free propagator ξ_{12}^0 has the same definition as Eq. (3.44), except that q_{12} is now replaced by g_{12}^0. Equation (3.39) is a generalization of Eq. (3.34) to order $\Phi^{1/2}$. We should note here that if one makes a Markov approximation in Eq. (3.30b), Eq. (3,.39) exactly reduces to the kinetic equation previously obtained in Ref. [19], where $\beta=1$.

Because of the spatial inhomogeneities of the single distribution function $f(R,\mathbf{r};t)$, it is not easy for us to solve Eq. (3.39) analytically. In the following, therefore, we discuss only a simple case where the spatial inhomogeneities of $f(R;\mathbf{r};t)$ are neglected.

D. A Fokker-Planck type kinetic equation for $f(R,t)$

We first introduce the reduced time by

$$\tau=t/T_0 ,$$ (3.45)

where $T_0=R_0^3/\alpha D$. Putting $f(R,\mathbf{r};t)=f(R,\tau)$ and using Eq. (2.8), we obtain

$$f(R,\tau)=\frac{n(\tau)}{\langle R\rangle(\tau)}F(\rho,\tau) ,$$ (3.46)

with the relative-droplet-size distribution function $F(\rho,\tau)$, which satisfies the boundary conditions,

$$\int_0^\infty F(\rho)d\rho=\int_0^\infty \rho F(\rho)d\rho=1 ,$$ (3.47)

where $\rho=R/\langle R\rangle=a/\langle a\rangle$. Use of Eqs. (3.33) and (3.44) then leads to

$$\xi_{12}(t)=\frac{\langle R\rangle}{|\mathbf{r}_{12}|}\exp[-|\mathbf{r}_{12}|/l(\tau)] ,$$ (3.48)

with the time-dependent screening length,

$$l(\tau)=[4\pi n(\tau)\langle R\rangle(\tau)]^{-1/2} .$$ (3.49)

By using Eqs. (3.27) and (3.40), we thus find the screening terms,

$$\lambda(R,\tau)=1-\beta(\tau)\rho ,$$ (3.50)

$$v(R,\mathbf{r};\tau)=(3\Phi/\mu_3)^{1/2}\beta(\tau)\rho(\mu_2-\rho) ,$$ (3.51)

with the coefficient,

$$\beta(\tau)=\langle a\rangle(\tau)\left[1+3\int_0^{\tau/\tau_s}v(\tau_s x)\langle\lambda\rangle(\tau_s x)dx\right] ,$$ (3.52)

where $v(\tau)$ is the normalized number density given by

$$v(\tau)=n(\tau)/n(0) .$$ (3.53)

Here the reduced screening time τ_s is given by

$$\tau_s=(T_s/T_0)=[Q\langle a\rangle(0)^3/\Phi_0] .$$ (3.54)

The second term of Eq. (3.52) represents the screening

effect of order Φ^0 and becomes important on the time scale of order τ_s. Here $\mu_n(\tau)=\langle\rho^n\rangle(\tau)$ denotes the nth moment of the relative droplet radius ρ, where the brackets denote the average over the relative-droplet-size distribution function $F(\rho,\tau)$,

$$\langle\cdots\rangle(\tau)=\int d\rho\cdots F(\rho,\tau) . \tag{3.55}$$

As is shown in Appendix D, we can transform the correlation term into the following simpler form:

$$\Lambda(R,r;\tau)f(R,\tau)$$
$$=(3\Phi/\mu_3)^{1/2}\left[-\rho\lambda+\frac{\langle\lambda^2\rangle}{\beta\mu_{-1}}\rho\frac{\partial}{\partial\rho}\frac{1}{\rho}\right]f(R,\tau) , \tag{3.56}$$

where in order to derive Eq. (3.56) from Eq. (3.29), we have neglected the derivatives in $(\partial/\partial\rho)$ higher than second order. Thus Eq. (3.39) reduces to the following Fokker-Planck type kinetic equation for $f(R,t)$:

$$\frac{\partial}{\partial\tau}f(R,\tau)=\frac{1}{\langle a\rangle^3}\frac{\partial}{\partial\rho}\frac{1}{\rho^2}\left[\lambda(\tau)+(3\Phi/\mu_3)^{1/2}\left[-\rho\langle\rho\lambda\rangle+\frac{\langle\lambda^2\rangle}{\beta\mu_{-1}}\rho\frac{\partial}{\partial\rho}\frac{1}{\rho}\right]\right]f(R,\tau) , \tag{3.57}$$

where the volume fraction Φ is given by

$$\Phi(\tau)=(Q/\tau_s)\nu(\tau)\langle a^3\rangle(\tau) . \tag{3.58}$$

Use of Eq. (3.57) then leads to the growth laws,

$$\frac{d}{d\tau}\langle a^3\rangle=\mu_3 K(\tau)-3\langle\lambda\rangle[1-(3\Phi/\mu_3)^{1/2}/\beta] , \tag{3.59a}$$

$$\frac{d}{d\tau}\ln\nu(\tau)=-K(\tau)/\langle a\rangle^3 , \tag{3.59b}$$

with the coarsening rate,

$$K(\tau)=\lim_{\rho\to0}F(\rho,\tau)/\rho^2 . \tag{3.60}$$

Equation (3.57) is a kinetic equation for the single-droplet-size distribution function $f(R,\tau)$ and describes the kinetics of phase separation over the entire time region after the nucleation stage. Since it does not contain any adjustable parameters, the distribution $f(R,\tau)$ can be obtained by solving it self-consistently so as to satisfy the boundary conditions (3.47). This will be discussed in Sec. III F.

E. Three characteristic stages and crossovers

We here discuss the asymptotic behavior of Eqs. (3.57) and (3.59). As is seen from Eqs. (3.59), there are two kinds of growth mechanisms. One is the direct growth from the supersaturated solution, which is described by the term $\langle\lambda\rangle$. This mechanism does not change the number density ν and increases the volume fraction Φ. Another is the growth due to the coarsening, where the larger droplets grow at the expense of the smaller ones which disappear. This is described by the coarsening rate K. This mechanism leads to the reduction of the number density but does not change the volume fraction. Thus there are three characteristic stages after the nucleation stage, depending on the asymptotic properties of K and $\langle\lambda\rangle$. After the nucleation stage, on the time scale of order T_0 (or $\tau=1$), the many-body effects are not important and hence the droplets grow directly and independently from the supersaturated solution, where the number den-

sity remains constant. This is the growth stage $[G]$ and continues up to the screening time T_s (or τ_s) when the screening effect of order Φ^0 becomes important. Since the integral on the right-hand side of Eq. (3.52) and the correction term of Eq. (3.57) can be negligible, we thus find

$$F(\rho,\tau)=\delta(\rho-1) . \tag{3.61}$$

The growth laws for the time region $1<\tau<\tau_s$ are then given by

$$K=0, \quad \langle\lambda\rangle=1-\langle a\rangle , \tag{3.62}$$

where the coarsening does not play any role in growth. Use of Eqs. (3.59) and (3.62) then leads to the temporal power laws

$$\langle a\rangle^2\sim2\tau, \quad \nu=1, \quad \Phi\sim\tau^{3/2} . \tag{3.63}$$

For $\tau\geq\tau_s$, the droplets separated by a distance of order l start to interact through the diffusive long-range interactions among droplets and hence their growth is no longer independent. Thus two kinds of growth mechanisms play an important role in the kinetics of droplet growth, where the coarsening starts to decrease the number density ν and the growth is slowed down by the long-range interactions. This is the intermediate stage $[I]$ and continues up to the coarsening time T_c (or $\tau_c=T_c/T_0$) when the growth from the solution is over, where $\langle\lambda\rangle\sim0$. As is shown in Appendix E, the coarsening time τ_c is given by

$$\tau_c=T_c/T_0=\tau_s/(K_\infty\mu_3^\infty\nu_s)^3 , \tag{3.64}$$

where $K_\infty=K(\infty)$, $\mu_3^\infty=\mu_3(\infty)$, and $\nu_s=\nu(\tau_s)$. In this stage the relative-droplet-size distribution function $F(\rho,\tau)$ depends on time explicitly. As is shown in Appendix E, we obtain the growth law for the time region $\tau_s\leq\tau<\tau_c$,

$$K\sim-\langle\lambda\rangle\sim\langle a\rangle^{-1} . \tag{3.65}$$

Hence two kinds of growth mechanisms compete with each other. Use of Eqs. (3.59) and (3.65) then leads to

$$\langle a \rangle \sim \tau^{1/4}, \quad \nu \sim \tau^{-2/3}, \quad \Phi \sim \tau^{1/12} \ . \tag{3.66}$$

For $\tau \geq \tau_c$, the coarsening stage $|C|$ starts, where the growth is governed only by the coarsening mechanism. As is shown in Appendix E, we have the growth laws for the time region $\tau \geq \tau_c$,

$$K = K_\infty [1 + c_1 \langle a \rangle^{-1}] + O(\langle a \rangle^{-2}) \ ,$$
$$\langle \lambda \rangle = -(\mu_3^\infty K_\infty /9)\langle a \rangle^{-1} + O(\langle a \rangle^{-2}) \ , \tag{3.67}$$

where c_1 is a positive constant to be determined. Then we have $|\langle \lambda \rangle /K| \ll 1$ for $\tau \geq \tau_c$. Hence the coarsening dominates the growth here. Use of Eqs. (3.59) and (3.67) thus leads to

$$\langle a \rangle^3 = K_\infty \tau [1 + A_1 (K_\infty \tau)^{-1/3}] \ ,$$
$$\nu = (\tau_s / \mu_3^\infty)(K_\infty \tau)^{-1}[1 - A_2 (K_\infty \tau)^{-1/3}] \ , \tag{3.68}$$
$$\Phi = Q[1 - (K_\infty \tau)^{-1/3}] \ ,$$

where $A_1 = \frac{3}{2}(c_1 + \frac{1}{3})$ and $A_2 = \frac{3}{2}(c_1 + 1)$. Therefore, this stage is further decomposed into two stages: the transient stage with the time region $\tau_c < \tau \ll \tau_L$, where Φ is still increasing slowly in time, and the late stage with $\tau_L < \tau$, where $\Phi = Q$. Here $\tau_L = 0.02^{-3}/K_\infty$ is the late stage time over which the deviation of Φ from Q becomes less than 2%. Thus the relative-droplet-size distribution function $F(\rho, \tau)$ still depends on time through volume fraction Φ, leading to $F(\rho, \tau) = F_c(\rho, \Phi)$. On the one hand, in the late stage the growth laws are given by

$$K = K_\infty , \quad \langle \lambda \rangle = 0 \quad (\beta = 1) \ ,$$
$$\langle a \rangle^3 = K_\infty \tau , \quad \nu = (\tau_c / \mu_3^\infty)(K_\infty \tau)^{-1} \ . \tag{3.69}$$

The distribution function $F_c(\rho, \Phi)$ thus reaches the time-independent scaling function $F_L(\rho, Q)$, which is given by the solution of the second-order differential equation,

$$\left[4 + \rho \frac{d}{d\rho} \right] F_L(\rho)$$

$$= - \left[\frac{3}{K_\infty} \right] \frac{d}{d\rho} \frac{1}{\rho^2} \left[1 - \rho + \left[\frac{3Q}{\mu_3^\infty} \right]^{1/2} \frac{(\mu_2^\infty - 1)}{\mu_{-1}^\infty} \right.$$

$$\left. \times \left[\mu_{-1}^\infty \rho + \rho \frac{d}{d\rho} \frac{1}{\rho} \right] \right]$$

$$\times F_L(\rho) \ , \tag{3.70}$$

where Eqs. (3.46) and (3.69) have been used to derive Eq. (3.70) from Eq. (3.57). Equation (3.70) is a new equation to describe the late stage process.

As discussed below, the screening effect of order Φ^0 turns out to alter the qualitative behavior of the temporal power laws for the radius $\langle a \rangle$, the number density ν, and the volume fraction Φ, and causes the two crossovers of the time exponents around τ_s and τ_c. Define the time exponents η_R, η_n, and η_Φ by

$$\langle a \rangle \sim \tau^{\eta_R}, \quad \nu \sim \tau^{-\eta_n}, \quad \Phi \sim \tau^{\eta_\Phi} \ , \tag{3.71}$$

where $\eta_\Phi = 3\eta_R - \eta_n$. Then their theoretical values are listed in Table I. On the other hand, the correlation effect of order $\Phi^{1/2}$ does not alter such a qualitative behavior but changes the quantitative behavior of the distribution function $f(R, \tau)$, leading to the volume fraction dependence (see Figs. 2, 5, and 6).

F. Numerical solutions

We now solve the second-order differential equation (3.57) self-consistently so as to satisfy Eq. (3.47). As the initial conditions, we first choose the Gaussian-type distribution function $f(R, 0)$ with the average $\langle a \rangle(0) = 1.1$ and the variance 10^{-5}, which satisfies $f/a^2 \to 0$ as $a \to 0$. Next we choose the initial value of the volume fraction under such a condition that the conservation law $\Phi = Q$ must be satisfied in the late stage. Thus we find $\Phi_0 = 6.47 \times 10^{-5}$ ($Q = 0.01$) and 1.47×10^{-3} ($Q = 0.1$). Then the values of τ_s, τ_c, and τ_L are estimated analytically (see Table II).

In Fig. 1 we show the time evolution of the relative-droplet-size distribution function $F(\rho, \tau)$ at $Q = 0.1$ for various reduced times; $\tau = 30$, 300, 3000, and 10^5. The scaling function $F_L(\rho)$, which is the solution of Eq. (3.70), is also shown by the dotted line for comparison. In Fig. 2 a log-log plot of the peak height $F_M(\tau)$ of $F(\rho, \tau)$ vs τ is shown for $Q = 0.01$ and 0.1. It decreases in time and reaches the constant value at the late stage. In the transient stage of coarsening, the distribution function $F(\rho, \tau)$ still depends on time through Φ and reaches the scaling function $F_L(\rho)$ in the late stage. In Fig. 3 the volume fraction dependence of $F(\rho, \tau)$ is also shown at $\tau = 10^5$ for $Q = 0.01$ and 0.1. As Q increases, the distribution function becomes broader and flatter, where its peak position shifts to the right.

In order to confirm the theoretical results obtained by Eq. (3.57), we can also simulate Eq. (2.5) directly. In Fig. 4 we show the histogram of $F(\rho, \tau)$ at $Q = 0.1$ for $\tau = 300$

TABLE I. Values of time exponents for stages $[G]$, $[I]$, and $[C]$.

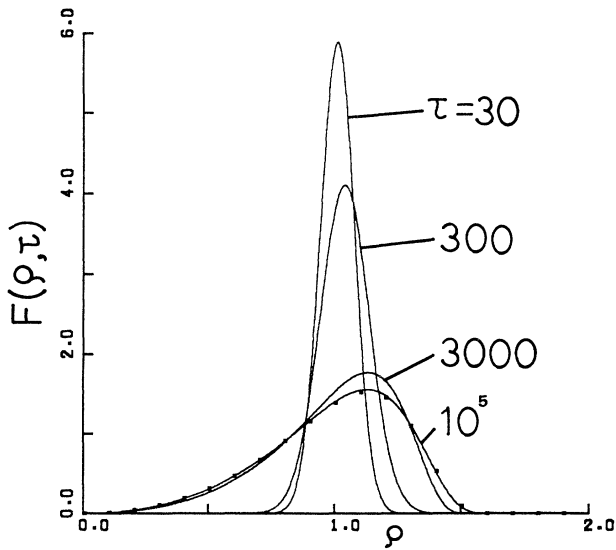| Stage	Time exponents				
	η_s	η_k	η_R	η_n	η_Φ
$[G]$	3	0	$\frac{1}{2}$	0	$\frac{3}{2}$
$[I]$	$\frac{25}{36}$	$\frac{2}{9}$	$\frac{1}{4}$	$\frac{2}{3}$	$\frac{1}{12}$
	$(=0.694)$	$(=0.222)$	$(=0.250)$	$(=0.667)$	$(0=0.083)$
$[C]$	1	$\frac{1}{3}$	$\frac{1}{3}$	1	0

FIG. 1. Time evolution of the relative-droplet-size distribution function $F(\rho,\tau)$ at $Q=0.1$ for various times. The dotted line indicates the time-independent scaling solution $F_L(\rho)$.
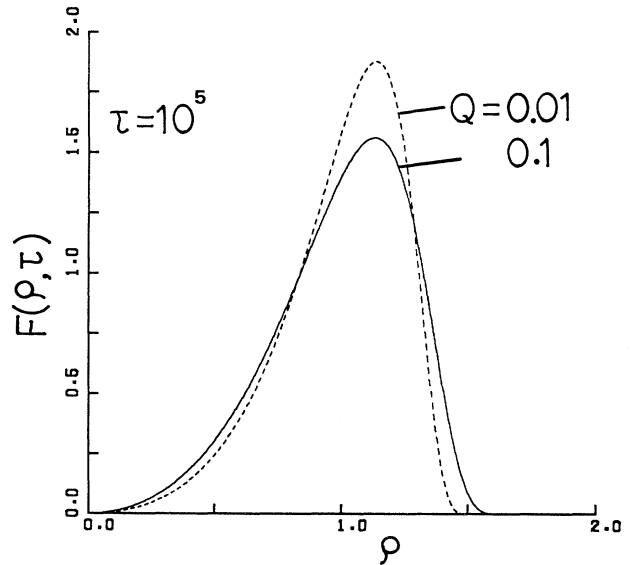

FIG. 3. Volume-fraction dependence of the relative-droplet-size distribution function $F(\rho,\tau)$ at $\tau=10^5$ for $Q=0.01$ (broken line) and 0.1 (full line).

and 10^5. The analytical results are also shown by the solid lines for comparison. We see that the error introduced by the approximations has no effect on the first-order correction.

In Figs. 5(a), 5(b), and 5(c) we show the time evolution of the normalized number density $\nu(\tau)$, the normalized volume fraction $\Phi(\tau)/Q$, and the growth rate $(d\langle a^3 \rangle/d\tau)$ for $Q=0.01$ and 0.1, respectively, where the slopes of the lines indicate the theoretical values of the exponents. In Fig. 6 we also show the time evolution of the reduced average droplet radius $\langle a \rangle(\tau)$ for $Q=0.01$ and 0.1. As Q increases, the magnitude of $\langle a \rangle$ becomes larger because of the correction term of order $\Phi^{1/2}$. In Fig. 7 the coarsening rate $K(\tau)$ is plotted versus τ for $Q=0.01$ and 0.1 on a logarithmic scale, where $K_\infty=0.59$ for $Q=0.01$ and $K_\infty=0.78$ for $Q=0.1$. As is seen from Figs. 5–7, the power-law behavior given by Eq. (3.71) is satisfied and the crossovers are thus observed around τ_s and τ_c, leading to the three characteristic stages.

IV. A LINEAR EQUATION FOR THE DYNAMIC STRUCTURE FUNCTION

Thus far, we have concentrated on the deterministic equation for $f(R,t)$. In the present section, we investigate the properties of the fluctuations around the deterministic motion and thus derive an equation of motion for the structure function.
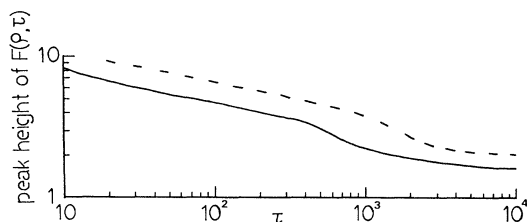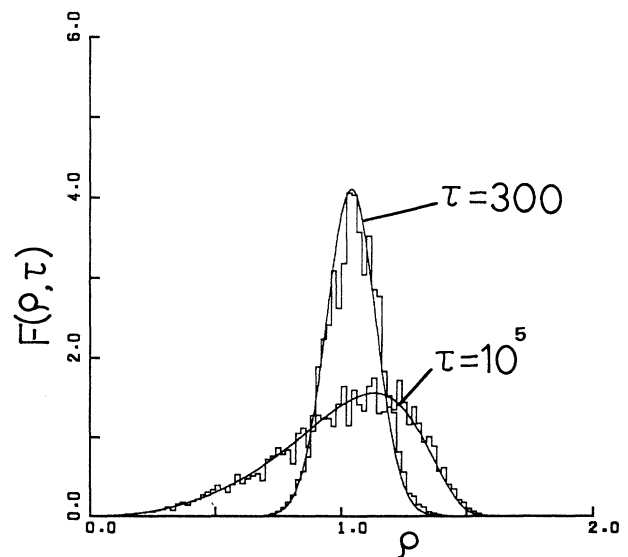

FIG. 2. A log-log plot of the peak height $F_M(\tau)$ vs τ for $Q=0.01$ (broken line) and 0.1 (full line). The line has a slope of $-1/5$ at stage $[G]$, $-1/6$ at stage $[I]$, and 0 at stage $[C]$.

FIG. 4. Time evolution of the relative-droplet-size distribution function $F(\rho,\tau)$ at $Q=0.1$ for $\tau=300$ and 10^5. The histograms indicate the results of the numerical simulation and the solid curves the analytical results (cf. Fig. 1).
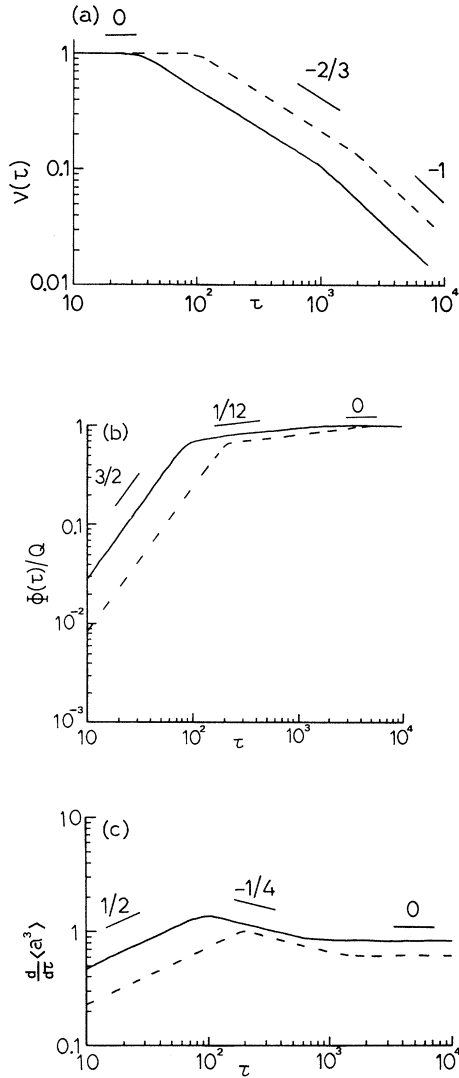
FIG. 5. (a) A log-log plot of the normalized number density $v(\tau)$ vs τ. (b) A log-log plot of the normalized volume fraction $\Phi(\tau)$ vs τ. (c) A log-log plot of the growth rate $(d\langle a^3 \rangle/d\tau)$ vs τ. The broken line indicates the result for $Q=0.01$ and the full line for $Q=0.01$. The slopes of the lines indicate the theoretical values of the time exponents.
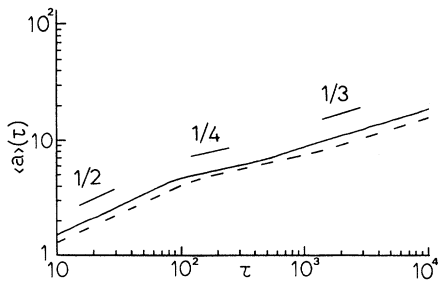

FIG. 6. A log-log plot of the reduced average droplet radius $\langle a \rangle(\tau)$ vs τ. Details are the same as in Fig. 5.

TABLE II. The analytical estimations of τ_s, τ_c, and τ_L for $Q=0.01$ and 0.1 at $\langle a \rangle(0)=1.1$.

Q	τ_s	τ_c	τ_L
0.01	206	1288	2.1×10^5
0.1	91	361	1.6×10^5

A. A linear variance equation up to order $\Phi^{1/2}$

The fluctuations are described by the variance $\chi(1,2;t)$. Hence we first derive an asymptotic equation for χ from Eq. (3.24) in the scaling limit $S \to \infty$. Use of Eqs. (2.13), (3.11), (3.12), and (3.35) leads, on the space-time scale (l,T), to

$$\frac{\partial}{\partial t}\chi_k(R_1,R_2;t)= \alpha D (1+e_{12})\frac{\partial}{\partial R_2} \frac{1}{R_2^2} m (q,\rho_2;\tau)$$

$$\times \chi_k(R_1,R_2;t) , \qquad (4.1)$$

with the screening operator,

$$m (q,\rho_2;\tau)=\lambda(\rho_2,\tau)- \frac{\rho_2 F(\rho_2,\tau)}{q^2+1} \int d\rho_3\lambda(\rho_3,\tau)e_{32} , \qquad (4.2)$$

where we have neglected the spatial inhomogeneities of the single-droplet-size distribution function $f(R,\mathbf{r};t)$ to obtain Eq. (4.2). Here the dimensionless variable q is given by

$$q(\tau)=kl(\tau) \quad (k =|\mathbf{k}|) . \qquad (4.3)$$

On the time scale of order T, the variance equation (4.1) does not contain a source term. Hence the fluctuations are generated only by an initial randomness $\chi_k(R_1,R_2;\tau=0)$, which originates from thermal fluctuations. The fluctuations could also be generated by the correlation effect of order $\Phi^{1/2}$. We next investigate this.

Similarly to Eq. (3.38), on the time scale of order T', one can generalize Eq. (3.19) as

$$\chi_k(R_1,R_2;t)= \frac{3\Phi}{4\pi\langle a \rangle^5}\tilde{\chi} \left[q,\rho_1,\rho_2; \frac{t}{T},\frac{t}{T'} \right] . \qquad (4.4)$$

As is shown in Appendix C, similarly to the derivation of Eq. (3.39), we thus obtain, in the dimensionless form,
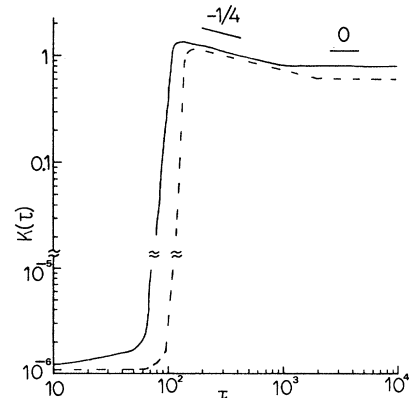

FIG. 7. A log-log plot of the coarsening rate $K(\tau)$ vs τ. Details are the same as in Fig. 5.

$$\frac{\partial}{\partial\tau}\chi_k(R_1,R_2;\tau)=\frac{(1+e_{12})}{\langle a\rangle^3}\frac{\partial}{\partial\rho_2}\frac{1}{\rho_2^2}$$

$$\times\left\{\int_0^\infty d\rho_3 H_q(\rho_2,\rho_3;\tau)\chi_k(R_3,R_1;\tau)\right.$$

$$\left.+\frac{(3\Phi/\mu_3)^{3/2}}{4\pi\langle a\rangle^5}E_q(\rho_2,\rho_1;\tau)\right\},$$

$$(4.5)$$

with the linear coefficient,

$$H_q(\rho_2,\rho_3;\tau)=m(q,\rho_2;\tau)\delta(\rho_2-\rho_3)$$

$$+(3\Phi/\mu_3)^{1/2}[v_q(\rho_2,\rho_3;\tau)+\Lambda_q(\rho_2,\rho_3;\tau)],$$

$$(4.6)$$

where $v_q(q,\rho_2,\rho_3)$ is the screening term given by

$$v_q(\rho_2,\rho_3;\tau)=\beta(\tau)\rho_3(\mu_2-\rho_3)\left[\delta(\rho_3-\rho_2)-\frac{\rho_2 F(\rho_2,\tau)}{q^2+1}\right],$$

$$(4.7)$$

and $\Lambda_q(\rho_2,\rho_3)$ is the correlation term given by

$$\Lambda_q(\rho_2,\rho_3;\tau)=-\left[\rho_3\lambda(\rho_3)+\frac{\langle\lambda^2\rangle}{\beta\mu_{-1}}\frac{1}{\rho_3}\frac{\partial}{\partial\rho_3}\rho_3\right]$$

$$\times\left[\delta(\rho_3-\rho_2)-\frac{\rho_2 F(\rho_2,\tau)}{q^2+1}\right].\quad(4.8)$$

Here the source term E_q is given by

$$E_q(\rho_2,\rho_1;\tau)=-\Lambda_q(\rho_2,\rho_1;\tau)F(\rho_1,\tau)-\frac{1}{2\pi^2}\int dp\frac{\rho_2}{p^2+1}\left[\left[1-\frac{F(\rho_2)}{q^2+1}\int d\rho_3\rho_3 e_{32}\right]\tilde{G}_2(q-p,\rho_1,\rho_2;\tau)\right.$$

$$\left.+\left[\delta(\rho_1-\rho_2)-\frac{F(\rho_2)}{q^2+1}\right]\int d\rho_3\tilde{G}_2(p,\rho_1,\rho_3;\tau)e_{31}\right]\lambda(\rho_1),\quad(4.9)$$

where the scaled pair-correlation function $\tilde{G}_2$ is given by

$$\tilde{G}_2(q,\rho_1,\rho_2;\tau)=-\frac{1}{q^2+1}\int_0^\infty d\tau\exp\left[\tau(1+e_{12})\frac{\partial}{\partial\rho_2}\frac{1}{\rho_2^2}m(q,\rho_2)\right](1+e_{12})\lambda(\rho_1)\frac{\partial}{\partial\rho_2}\frac{1}{\rho_2}F(\rho_1,\tau)F(\rho_2,\tau).\quad(4.10)$$

Equation (4.5) is a generalization of Eq. (4.1) to order $\Phi^{1/2}$ and describes the fluctuations with the length scale of order l over the entire time region. We note here that the Fourier transform of the coefficient $H_q(\rho_2,\rho_3)$ is simply related to the term $J_1(2)$ through $H(2,3)=\delta J_1(2)/\delta f(3)$. This is because Eq. (4.5) is an equation for the fluctuations which complements the deterministic equation (3.39).

The variance equation (4.5) has the source term E_q, which is related to the correlation term $\Lambda(1)$ through the pair correlation G_2. On the time scale of order T', therefore, the fluctuations are generated not only by the initial randomness but also by the dynamic many-body (spatial correlation) effect. Thus the effects of those fluctuations on the dynamics of the structure function $S(k,t)$ are expected to be different from each other.

B. A linear non-Markov equation for the structure function

We now derive a linear equation for the dynamic structure function $S(k,t)$ from the linear variance equation (4.5).

We first define the function u_p by

$$u_p(\rho)=\rho^3\psi(\rho p),\quad(4.11)$$

with the dimensionless variable,

$$p=k\langle R\rangle\quad(k=|\mathbf{k}|),\quad(4.12)$$

where ψ is given by Eq. (2.15). It is then convenient to introduce a matrix notation as $\underline{u}_p$ for the column matrix $\{u_p(\rho)\}$ and $\underline{H}_q(\tau)$ for the matrix whose (ρ,ρ') component is given by $H_q(\rho,\rho',\tau)$. Use of Eqs. (2.14) and (4.5) thus leads to

$$\frac{d}{dt}S(k,\tau)=2\langle a\rangle^5\left[\frac{4\pi}{3}\right]^2$$

$$\times\left[\underline{u}_p^*\cdot\underline{\hat{Q}}\cdot\underline{H}_q(\tau)\cdot\underline{\chi}_k(\tau)\cdot\underline{u}_p\right.$$

$$\left.+\frac{(3\Phi/\mu_3)^{3/2}}{4\pi\langle a\rangle^5}\underline{u}_p^*\cdot\underline{\hat{Q}}\cdot\underline{E}_q\cdot\underline{u}_p\right],\quad(4.13)$$

where $|\underline{\hat{Q}}|_{\rho b}=(\partial/\partial\rho)\rho^{-2}\delta(\rho-b)$, and the asterisk denotes the Hermitian conjugate. In order to derive an equation for $S(k,\tau)$ from Eq. (4.13), we introduce a projection operator matrix $\underline{P}$ by

$$\underline{P}\cdot\underline{A}=(\underline{u}_p^*\cdot\underline{A}\cdot\underline{u}_p)\underline{E},\quad(4.14)$$

where $|\underline{E}|_{\rho b}=\delta(\rho-b)F(\rho,\tau)/\langle u_p^2\rangle$, and $\underline{A}$ is an arbitrary matrix. Then we have $[\underline{P}\cdot\underline{\chi}_k]_{\rho b}=(3/4\pi)^2\delta(\rho-b)S_k(\tau)/\langle R\rangle^8\langle u_p^2\rangle$. As is shown in Appendix F, the projection operator method then leads to the following linear non-Markov equation

for $S(k,\tau)$:

$$\frac{d}{d\tau}S(k,\tau)=\frac{2}{\langle a \rangle^3}\left[h(p,q,\tau)S(k,\tau) \right.$$

$$\left. -\int_0^{\tau}\Theta(p,q,\tau;s)S(k,\tau-s) \right]$$

$$+2\left[\frac{4\pi\Phi}{3\mu_3}\right]\Gamma(p,q,\tau) , \qquad (4.15)$$

with the instantaneous term,

$$h(p,q,\tau)=-\frac{3}{\langle u_p^2 \rangle}\int_0^{\infty}db\langle u_p(\rho)H_q(b,\rho,\tau)\rangle\omega(bp) ,$$

$$(4.16)$$

and the memory term,

$$\Theta(p,q,\tau;s)=\frac{1}{\langle u_p^2 \rangle}\int_0^{\infty}db\langle u_p(\rho)H_q(b,\rho,\tau)\rangle$$

$$\times\frac{1}{b^2}\frac{\partial}{\partial b}\zeta_{pq}(b,\tau;s) , \qquad (4.17)$$

where the source term $\Gamma(p,q,\tau)$ is given by

$$\Gamma(p,q,\tau)=\int_0^{\tau}\Theta(p,q,\tau;s)\langle u_p^2 \rangle(\tau-s)ds$$

$$+(3\Phi/\mu_3)^{1/2}B(p,q,\tau) , \qquad (4.18)$$

with the term related to the correlation effect

$$B(p,q,\tau)=\underline{u}_p^*\cdot\hat{\underline{Q}}\cdot\underline{E}_q\cdot\underline{u}_p . \qquad (4.19)$$

Here $\omega(\theta)=\sin\theta/\theta$, $q=kl$, and $p=k\langle R \rangle$.

The function $\zeta_{pq}(\rho,\tau;s)$ represents a fluctuating force and is given by the ρ component of the following matrix:

$$\underline{\zeta}_{pq}(\tau;s)=\underline{V}_q(s)\cdot(\underline{1}-\underline{P}^*)\cdot\underline{H}_q^*(\tau)\cdot\hat{\underline{Q}}^*\cdot\underline{u}_p , \qquad (4.20)$$

with the propagator,

$$\underline{V}_q(s)=\exp[s(\underline{1}-\underline{P}^*)\cdot\underline{H}_q^*(\tau)\cdot\hat{\underline{Q}}^*] , \qquad (4.21)$$

where the fluctuating force $\zeta_{pq}(\rho,\tau;s)$ satisfies the orthogonality condition $\langle\zeta_{pq}(\rho,\tau;s)u_p(\rho)\rangle=0$.

Equation (4.15) is a new linear non-Markov equation for the structure function $S(k,t)$ which is valid over the entire time region. The source term Γ consists of two terms which are related to two kinds of fluctuations discussed before. The first term of Eq. (4.18) is related to the nonthermal fluctuations generated by the fluctuating force $\zeta_{pq}(\rho,\tau;s)$. This originates from the initial randomness $\chi_k(R_1,R_2;\tau=0)$ and exists even in the limit $Q\rightarrow0$. The second term is related to the nonthermal fluctuations generated by the spatial correlations. This is of order $\Phi^{1/2}$ and vanishes in the limit $Q\rightarrow0$.

C. A linear Markov equation for $S(k,\tau)$

Since Eq. (4.15) does not contain any adjustable parameters, one may solve it under an appropriate initial condition to obtain the time evolution of $S(k,\tau)$. However, it is not easy to calculate it since it is a non-Markov equation and also the source term $\Gamma(p,q;\tau)$ contains the higher-order derivatives in operator $(\partial/\partial\rho)$ to be calculated. Hence we here make the following approximations to transform Eq. (4.15) into a simpler form. First, the time scale of the fluctuating force $\zeta_{pq}(\rho,\tau;s)$ is assumed to be much smaller than that of $S(k,\tau)$. Then one can make a Markov approximation in Eq. (4.15) after stage $|G|$. Second, in order to find the more tractable forms for the memory term Θ and the source term B, we employ a similar approximation to that used in the derivation of Eq. (3.56), where the derivatives in $(\partial/\partial\rho)$ higher than second order have been neglected. Thus we obtain

$$\frac{d}{d\tau}S(k,\tau)=\frac{2}{\langle a \rangle^3}[h(p,q,\tau)-\gamma(p,q,\tau)]S(k,\tau)$$

$$+2\left[\frac{4\pi\Phi}{3\mu_3}\right]\Gamma(p,q,\tau) , \qquad (4.22)$$

with the instantaneous term $h(p,q;\tau)=Z^{(1)}(p,q;\tau)$ and the damping term $\gamma(p,q;\tau)=Z^{(2)}(p,q;\tau)$, which are given by

$$Z^{(n)}(p,q;\tau)=-\frac{3}{\langle u_p^2 \rangle}\left[\langle\rho^3\lambda X^{(n)}\rangle+(3\Phi/\mu_3)^{1/2}\left[(\beta\mu_2-1)\langle\rho^4 X^{(n)}\rangle-\frac{\langle\lambda^2\rangle}{\beta\mu_{-1}}\langle\rho^2 Y^{(n)}\rangle\right]\right] , \qquad (4.23)$$

where

$$X^{(n)}(\rho p,q)=\psi(\rho p)\left[\omega(\rho p)-\langle\rho\omega(\rho p)\rangle\frac{1+2(n-1)q^2}{(q^2+1)^n}\right] , \qquad (4.24)$$

$$Y^{(n)}(\rho p,q)=\psi(\rho p)\left[\cos(\rho p)-\langle\rho\omega(\rho p)\rangle\frac{1+2(n-1)q^2}{(q^2+1)^n}\right] . \qquad (4.25)$$

The source term Γ is given by

$$\Gamma(p,q,\tau)=\langle u_p^2 \rangle\gamma(p,q,\tau)+(3\Phi/\mu_3)^{1/2}B(p,q,\tau) , \qquad (4.26)$$

$$B(p,q,\tau)=-3\left[\langle\rho^4\psi\lambda\rangle\langle\rho\omega\rangle q^2/(q^2+1)+2\langle\rho^4\lambda X^{(1)}\rangle+\frac{\langle\lambda^2\rangle}{\beta\mu_{-1}}\{3\langle\rho^2\omega X^{(1)}/\psi\rangle+2\langle\rho^2 Y^{(1)}\rangle\}\right] . \qquad (4.27)$$

Here we should note that the Markov source term (4.26) is valid on the time region after the stage $[G]$. In order to discuss the growth stage process, therefore, one should use the non-Markov source term (4.18) without the correction term. In fact, at stage $[G]$, the source term Γ is given by

$$\Gamma(p,q,\tau) = \tau p^2 [\langle \rho^2 \lambda^2 \psi^2 \rangle - \langle \lambda \psi \rangle \langle \rho^3 \lambda \psi \rangle /(q^2+1)]$$

$$+ 3\tau \langle a \rangle [\langle \rho \lambda \psi \omega \rangle - \langle \rho \lambda \psi \rangle \langle \rho \omega \rangle /(q^2+1) - \langle \rho^3 \lambda \psi \rangle \{ \langle \omega/\rho \rangle - \mu_{-1} \langle \omega \rho \rangle /(q^2+1)\} /(q^2+1)] . \quad (4.28)$$

D. Dynamical scaling and temporal power laws

We now investigate the asymptotic behavior of $S(k,\tau)$. Using Eq. (3.71) and taking a dimensional analysis of Eqs. (4.15), (4.22), (4.26), and (4.28), we thus find a scaling law,

$$S(k,\tau) = k_M^{-d} \Phi^\delta \Psi(k/k_M,\tau) , \quad (4.29)$$

with the peak position of $S(k,t)$ as a function of k,

$$k_M^{-1}(\tau) = c_2 \langle R \rangle /\Phi^{1/d} , \quad (4.30)$$

where $d=3$ here, and c_2 is a positive constant to be determined. Here $\delta=2$ for stage $[G]$ and $1/d$ for stages $[I]$ and $[C]$. From Eq. (1.1), therefore, the inverse of k_M is proportional to the average distance between nearest neighbors as

$$L = (\mu_3^{1/3}/c_2) k_M^{-1} . \quad (4.31)$$

The peak height of $S(k,\tau)$ is then given by $S_M = S(k=k_M,\tau)$. Introducing the exponents η_k and η_S by

$$k_M^{-1} \sim \tau^{\eta_k}, \quad S_M \sim \tau^{\eta_S} \Psi(1,\tau) , \quad (4.32)$$

and using Eqs. (4.29) and (4.30), we thus obtain the relation

$$\eta_k = \eta_R - \eta_\Phi/d, \quad \eta_S = d\eta_k + \delta\eta_\Phi . \quad (4.33)$$

The theoretical values of these exponents are listed in Table I. The scaling relation (4.29) holds over the entire time region after the nucleation stage. In stage $[C]$ the scaling function $\Psi(x,\tau)$ depends on time only through Φ and becomes independent of time in the late stage.

We next discuss the asymptotic behavior of the scaling function $\Psi(x,\tau)$ in two limiting cases; $x \ll 1$ ($p \ll q \ll 1$), and $x \gg 1$ ($q \gg p \gg 1$), where $x = k/k_M$. In the limit $x \ll 1$, we have $\langle \psi \rangle \sim 1$, $\langle \omega \rangle \sim 1$, and $\langle u_p^2 \rangle \sim \mu_6$. Since $X^{(1)} \sim Y^{(1)} \sim q^2$ and $X^{(2)} \sim Y^{(2)} \sim q^4$, we obtain $h \sim q^2$, $B \sim q^2$, and $\Gamma \sim q^4$. From Eqs. (4.15) and (4.22), we thus find the asymptotic form

$$\Psi(x,\tau) \sim x^4 \quad \text{for } x \ll 1 . \quad (4.34)$$

The x^4 dependence of the scaling function is caused by the nonthermal fluctuations generated by the fluctuating force $\zeta_{pq}(\rho,\tau;s)$. This agrees with the recent theories [25–28].

In the limit $x \gg 1$, we have $\langle \psi \rangle \sim p^{-2}$, $\langle \omega \rangle \sim p^{-1}$, $\langle \psi \omega \rangle \sim p^{-4}$, and $\langle u_p^2 \rangle \sim x^{-4}$. Therefore, we find $h \sim \gamma \sim p^0$, $B \sim p^{-4}$, and $\Gamma \sim p^{-2}$ for $[G]$ and p^{-4} for $[I]$ and $[C]$. Use of Eqs. (4.15) and (4.22) then leads to the asymptotic form

$$\Psi(x,\tau) \sim x^{-4} \quad \text{for } x \gg 1 . \quad (4.35)$$

The x^{-4} tail is known as Porod's law and results from the fact that the droplet interfaces are assumed to be sharp after the nucleation stage. We should remark that at the earlier stage the exponent must be different from -4 since the droplet surface is not expected to be smooth.

Finally we discuss the asymptotic behavior of the scaling function $\Psi(x,\tau)$ in the late stage where $\Phi=Q$. Putting $\Psi_L(x,Q) = (3\mu_3^\infty/4\pi Q)\Psi(x,\tau)$ and using Eqs. (4.22) and (4.29), we obtain

$$\left[3 + p\frac{d}{dp} \right] \Psi_L(x,Q)$$

$$= \left[\frac{6}{K_\infty} \right] [j(p,Q)\Psi_L(x,Q) + \Gamma(p,q)] , \quad (4.36)$$

with

$$j(p,Q) = -\frac{3\langle \rho\omega \rangle q^2}{\langle u_p^2 \rangle (q^2+1)^2}$$

$$\times \left[\langle \rho^3 \psi \lambda \rangle + \left[\frac{3Q}{\mu_3^\infty} \right]^{1/2} (\mu_2^\infty - 1) \right.$$

$$\left. \times \{ \langle \rho^4 \psi \rangle - \langle \rho^2 \psi \rangle /\mu_{-1} \} \right] , \quad (4.37)$$

where $\lambda = 1 - \rho$, $q = p(3Q/\mu_3^\infty)^{-1/2}$, and $\Gamma(p,q)$ is given by Eq. (4.26). This is a new equation for the scaling function $\Psi_L(x)$ in the late stage. From Eq. (4.36), we thus find the asymptotic solution

$$\Psi_L(x,Q) = (6/K_\infty) p^{-3} \int_0^P dy\, y^2 \Gamma(y,Q)$$

$$\times \exp \left[(6/K_\infty) \int_y^P dz\, j(z)/z \right] , \quad (4.38)$$

where $p = x(k_M \langle R \rangle) = xQ^{1/3}/c_2$.

E. Numerical results

Finally we discuss the numerical solution of the Markov equation (4.22). Figure 8 shows the plot of the structure function $S(k,\tau)$ vs kR_0 at $Q=0.1$ for times (a) up to 300 and (b) from 3000 to 10^4. With increasing times, the structure function becomes narrower with the peak position shifting towards small wave vector and the peak
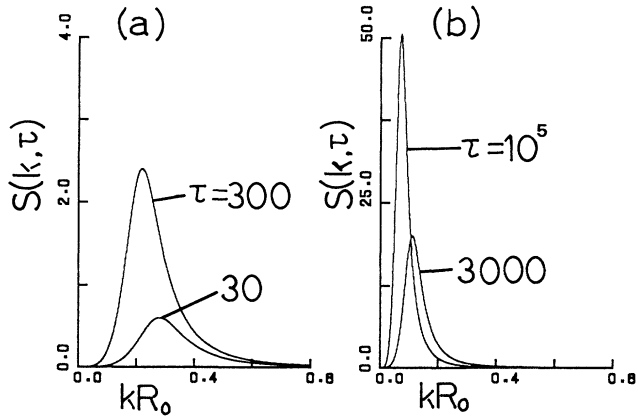
FIG. 8. Time evolution of the structure function $S(k,\tau)$ at $Q=0.1$ for times (a) up to 300 and (b) from 3000 to 10^4.

FIG. 10. A log-log plot of the peak height $S_M(\tau)$ vs τ. Details are the same as in Fig. 5.

height increasing rapidly. Figures 9 and 10 show a log-log plot of the reduced peak position $k_M R_0$ and the peak height S_M vs τ for $Q=0.01$ and 0.1, respectively. They satisfy the power-law behavior given by Eq. (4.32). The crossovers in the time exponents are also observed around τ_s and τ_c. In Fig. 11 a log-log plot of the structure function $S(k,\tau)$ vs kR_0 is shown at $Q=0.1$ for time (a) 300 (stage [I]) and (b) 3000 (stage [C]). Here the lines in small kR_0 have a slope of 4, while the lines in large kR_0 have a slope of -4. It is interesting to note here that a secondary maximum or a shoulder shows up for large kR_0 and becomes more evident at the later stage [34,35].

Finally, we discuss a normalized scaling function given by

$$\tilde{S}(x,\tau)=\frac{2\pi^2 k_M^3 S(k,\tau)}{\int_0^\infty dk\, k^2 S(k,\tau)}=\frac{2\pi^2\Psi(x,\tau)}{\int_0^\infty dx\, x^2\Psi(x,\tau)} , \quad (4.39)$$

where $x=k/k_M$. In Fig. 12 we show the plot of $\tilde{S}(x,\tau)$ vs x at $Q=0.1$ for different times $\tau=30$, 300, 3000, and 10^5. The time-independent scaling solution $\tilde{S}_L(x,Q)$, which is obtained from Eq. (4.38), is also shown by the dotted line for comparison. As time increases, the normalized scaling function becomes narrower with the in-
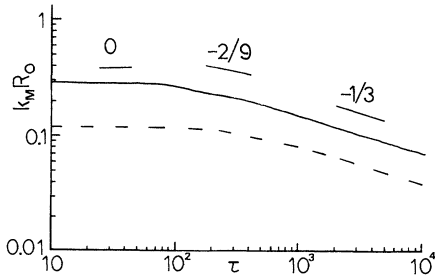
creasing peak height and reaches the scaling solution $\tilde{S}_L(x,Q)$ for $\tau>10^5$. In Fig. 13 we also show a log-log plot of the peak height of the scaling function, $\tilde{S}(1,\tau)$, vs τ for $Q=0.01$ and 0.1. It increases in time and reaches the constant value at the late stage. Figure 14 shows a log-log plot of the half width $\Delta_{1/2}(\tau)$ of the scaling function $\tilde{S}(x,\tau)$ vs τ for $Q=0.01$ and 0.1. As τ increases, the half width decreases. As Q increases, it also decreases. As is seen from Figs. 13 and 14, the scaling function $\tilde{S}(x,\tau)$ also becomes narrower and higher as Q increases. Finally, we should mention that the slope of $\frac{1}{2}$ of the peak height S_M in stage [G] is different from the theoretical value of 3. This is because the above numerical results in stage [G] were obtained by solving the Markov equation (4.22), which is not valid at stage [G]. In order to obtain the correct results in stage [G], therefore, one should solve the non-Markov equation (4.15) with Eq. (4.28) itself.

V. CONCLUSIONS

We have presented a systematic theory for the dynamics of phase separation in the quenched binary systems into the metastable states. In Sec. II we have first derived the basic equations for the radii of droplets, Eq. (2.5),
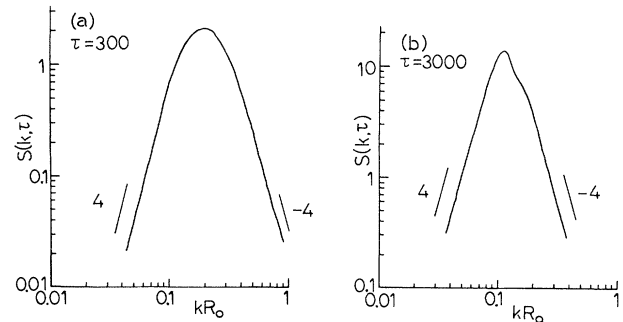

FIG. 9. A log-log plot of the reduced peak position $k_M R_0$ vs τ. Details are the same as in Fig. 5.

FIG. 11. A log-log plot of the structure function $S(k,\tau)$ vs kR_0 for (a) stage [I] ($\tau=300$) and (b) stage [C] ($\tau=3000$). The line has a slope of 4 for small k and -4 for large k.
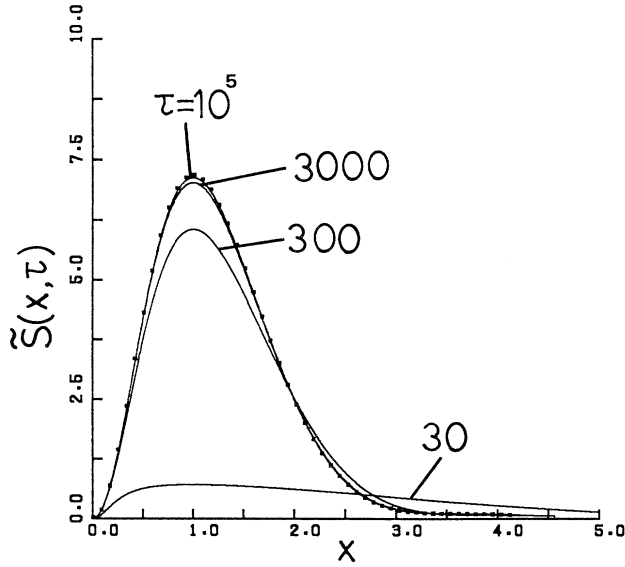
FIG. 12. Time evolution of the normalized scaling function $\tilde{S}(x,\Phi)$ at $Q=0.1$ for various times. The dotted line indicates the time-independent scaling function $\tilde{S}(x,Q)$.

FIG. 14. A plot of the half width $\Delta_{1/2}(\tau)$ vs τ for $Q=0.01$. Details are the same as in Fig. 5.

from the diffusion equation (2.1). In Sec. III we have then transformed them into the hierarchy equations for the multibody distribution functions. In order to truncate such equations, we have employed the systematic expansion method which enables us to carry out the space-time coarse graining in a manner consistent with the expansion in $\Phi^{1/2}$ and also to evaluate the relative magnitude of the fluctuations to the causal motion. Thus we have derived the Fokker-Planck type kinetic equation (3.57) and the linear variance equation (4.5), up to order $\Phi^{1/2}$. By using the projection operator method, we have further obtained the linear non-Markov equation (4.15) from the variance equation (4.5). Since Eqs. (3.57) and (4.15) did not contain any adjustable parameters, the time evolution of all macroscopic quantities is obtained by solving them under appropriate initial and boundary conditions. In order to confirm the theoretical results, in Sec. III we have also simulated the starting equation (2.5) directly and shown that the error introduced by the expansion in $\Phi^{1/2}$ has no effect on the first-order correction.
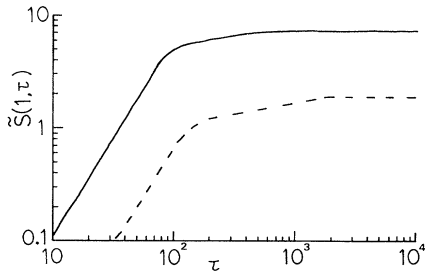

FIG. 13. A log-log plot of the peak height $\tilde{S}(1,\Phi)$ vs τ at $Q=0.1$. Details are the same as in Fig. 5.
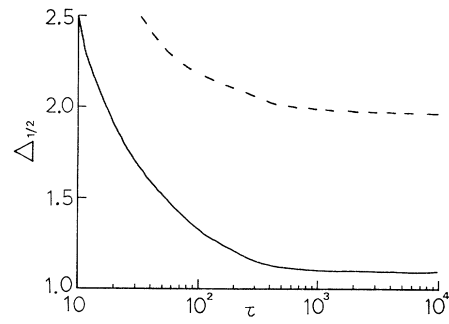
The diffusive long-range interactions among droplets were rigorously investigated, up to order $\Phi^{1/2}$. It has been shown that there are two kinds of many-body effects on droplet growth. One is the screening effect of order Φ^0 which is given by the second term of Eq. (3.51), and the other is the correlation effect of order $\Phi^{1/2}$ which is given by Eq. (3.56). The screening effect has been shown to cause significant changes in the growth of droplets qualitatively, leading to two types of crossovers in the time exponents of the average droplet radius $\langle R \rangle(t)$ and the number density $n(t)$. The first type around T_s is attributed to the transition from the free type to the fully interacting type growth from the supersaturated solution. The second type around T_c is attributed to the transition from the fully interacting type growth to the coarsening process. On the other hand, the correlation effect has been shown to alter only quantitative behavior of the distribution function $f(R,t)$ and the structure function $S(k,t)$, leading to their dependence on Q, and thus to cause appreciable corrections to their amplitudes obtained in the limit of the zero volume fraction (see Figs. 2 and 13).

There are several important features in the present theory. First, the three characteristic stages have been shown to exist after the nucleation stage. The first is the growth stage $[G]$ with the time region $T_0 \leq t < T_s$, where the free-type growth from the supersaturated solution dominates the system. The growth laws are given by $\langle R \rangle \propto t^{1/2}$, $n \propto t^0$, $\Phi \propto t^{3/2}$, and $k_M(\text{or } L) \propto t^0$. The average droplet radius grows rapidly and the number density remains constant. The second is the intermediate stage $[I]$ with $T_s \leq t < T_c$, where two growth mechanisms, the fully interacting type growth mechanism and the coarsening mechanism, compete with each other through the diffusive long-range interactions. The growth laws are given by $\langle R \rangle \propto t^{1/4}$, $n \propto t^{-2/3}$, $\Phi \propto t^{1/12}$, and $k_M \propto t^{-2/9}$. The growth is slowed down by the many-body effect. The last is the coarsening stage $[C]$ with $T_c \leq t$, where the Ostwald ripening dominates the system. The average radius and the number density obey the LSW growth law, $\langle R \rangle \propto t^{1/3}$, $n \propto t^{-1}$, $\Phi \propto t^0$, and $k_M \propto t^{-1/3}$. The coarsening stage has also been shown to be further decomposed into the transient stage with the time region $T_c \leq t \ll T_L$, where Φ is still increasing slowly in time [see Eq. (3.68)], and the late stage with $T_L < t$,

where $\Phi = Q$.

The second important feature is that the dynamical scalings, Eqs. (3.46) and (4.29), have been found to hold at each stage, where the time exponents are obtained analytically. In stage $[G]$, only one length $\langle R \rangle$ is relevant since $n(\tau)$ is constant. In stage $[I]$, two lengths $\langle R \rangle$ and L (or k_M^{-1}) are thus relevant since $n(\tau)$ depends on time, and hence the scaling functions $F(\rho, \tau)$ and $\Psi(x, \tau)$ depend on time explicitly. In stage $[C]$, only one length $\langle R \rangle$ is relevant. The scaling functions $F(\rho, \tau)$ and $\Psi(x, \tau)$ depend on time only through $\Phi(\tau)$ and become independent of time in the late stage.

The third important feature is that the linear equation for $S(k, t)$ has two kinds of source terms. One is the source term related to the nonthermal fluctuations generated by the fluctuating force $\zeta_{pq}(\rho, \tau; s)$. This is given by the first term of Eq. (4.18) and exists even in the limit $Q \to 0$. This leads to the x^4 dependence of the scaling function $\Psi(x)$ for small x. The other is the source term related to the nonthermal fluctuations generated by the spatial correlation. This is given by the second term of Eq. (4.18) and vanishes in the limit $Q \to 0$.

The fourth important feature is that the secondary maximum shows up in the structure function $S(k, \tau)$ for large k values at the later stage. This type of shoulder has been observed in experiments [35] as well as in theoretical [36] and numerical [37] calculations.

The final feature is that the present theory enables us to describe not only the earlier stage of phase separation but also the late stage in a simple manner. Recently, the late stage process was studied extensively by TKE [19] for finite volume fraction and their results agreed with experiments well [5,38]. In the late stage, however, the present theory provides much simpler results than theirs. In fact, the scaling function $F_L(\rho, Q)$ is determined by solving the second-order differential equation (3.70), and the scaling function $\Psi_L(x, Q)$ is given by the solution, Eq. (4.38), of Eq. (4.36). Although Eqs. (3.70) and (4.36) are simpler than those of TKE [19], all results obtained here agree with theirs within errors less than 1%.

ACKNOWLEDGMENTS

APPENDIX A: DERIVATION OF EQ. (2.5)

To eliminate the boundary conditions (2.2) and (2.3) from Eq. (2.1), we first write Eq. (2.1) as

$$\frac{\partial}{\partial t} C(\mathbf{r}, t) = D \nabla^2 C + \sum_{i=1}^{N} \int d\Omega_i \delta(\mathbf{r} - \mathbf{x}_i) \sigma_i(\Omega_i, t) . \quad \text{(A1)}$$

where σ_i denotes the strength of the interactions between the concentration field and the $i$the droplet at point Ω_i on its surface. By solving Eq. (A1), we obtain

$$C(\mathbf{x}_i, t) = C_b + \int_0^t dt' \int d\Omega_i^{-1} g_0(\mathbf{x}_i - \mathbf{x}_i', t - t') \sigma_i(\Omega_i', t')$$
$$+ \sum_{j (\neq i)}^{N} \int_0^t dt' \int d\Omega_j g_0(\mathbf{x}_i - \mathbf{x}_j, t - t') \sigma_j(\Omega_j, t') , \quad \text{(A2)}$$

where $g_0(\mathbf{x}, t) = \exp[-|\mathbf{x}|^2 / 4Dt] / (4\pi Dt)^{3/2}$. In order to solve this equation for σ_i, it is convenient to introduce the inverse propagator $g_{-1}(\Omega_i, \Omega_i')$ of the free propagator

$$g_0(\mathbf{x}_i - \mathbf{x}_i', t - t') = g_0(\Omega_i, \Omega_i'; t - t')$$

by

$$\int_{t'}^{t} dt'' \int d\Omega_i'' g_{-1}(\Omega_i, \Omega_i''; t, t') g_0(\Omega_i'', \Omega_i'; t'' - t')$$
$$= \delta(\Omega_i - \Omega_i') \delta(t - t') . \quad \text{(A3)}$$

On the time scale of order T, we then find

$$f d\Omega_i \int d\Omega_i' g_{-1}(\Omega_i, \Omega_i', t, t') = 2\delta(t - t')(4\pi DR_i) . \quad \text{(A4)}$$

By using Eq. (A3), we can invert Eq. (A2) to

$$\sigma_i(\Omega_i, t) = \int_0^t dt' \int d\Omega_i' g_{-1}(\Omega_i, \Omega_i'; t, t') \left[\rho_m(\alpha/R_i - \Delta_0) - \sum_{j (\neq i)} \int_0^{t'} dt'' \int d\Omega_j'' g_0(\mathbf{x}_0 - \mathbf{x}_j'', t' - t'') \sigma_i(\Omega_i'', t'') \right] . \quad \text{(A5)}$$

As shown in Sec. III, only the long-range spatial interaction over a distance of order l is important. Hence we have $g_0(\mathbf{x}_{ij}, t - t') = g_0(\mathbf{x}_{ij}, t - t') + O(\langle R \rangle / l)$. On the length scale of order l, use of Eqs. (2.4) and (A2)–(A5) thus leads to Eq. (2.5).

APPENDIX B: DERIVATION OF EQ. (3.26)

By inserting Eq. (3.3) into Eq. (3.6), we first decompose the function I_m into the most-dominant term I_{m0} and the correction term ΔI_m,

$$I_m = I_{m0} + \Delta I_m , \quad \text{(B1)}$$

$$I_{m0}(1, \dots, m) = f(1) \cdots f(m) \lambda(m; t) . \quad \text{(B2)}$$

In order to find the explicit form of the correction term ΔI_m, we next expand it formally in powers of the free propagators g^0. Iterating Eq. (3.7), inserting it into Eq. (3.6) and using Eq. (B1), we then find

$$\Delta I_m = \{f(1,\ldots,m)-f(1)\cdots f(m)\}\lambda(m;t)$$

$$+\sum_{n=m+1}^{\infty}(-1)^{n-m}\int_0^t dt_{m+1}\int_0^{t_{m+1}}dt_{m+2}\cdots\int_0^{t_{n-1}}dt_n\int d(m+1)\cdots\int d(n)$$

$$\times R_m g_{mm+1}^0(t-t_{m+1})\cdots R_{n-1}g_{n-1n}^0(t_{n-1}-t_n)\lambda(n,t_n)F_n^m(1,t;\ldots;m,t;m+1,t_{m+1};\ldots;n,t_n)\,,$$

$$\text{(B3)}$$

with the function

$$F_n^m(1,t;\ldots;m,t;m+1,t_{m+1};\ldots;n,t_n)$$

$$=\sum_{\substack{i,j\\(i\neq j)}}^{m}\Theta(|\mathbf{r}_{ij}|-R_i-R_j)\prod_{k=m+1}^{n}\Theta(|\mathbf{r}_k-\mathbf{r}_{k-1}|-R_k-R_{k-1})\overline{N(1;t)\cdots N(m;t)\delta N(m+1;t_{m+1})\cdots\delta N(n;t_n)}\,,$$

$$\text{(B4)}$$

where $n\geq m+1$ and $m\geq 1$. Here the expansion in powers of g_{ij}^0 is merely formal since the higher-order terms are not necessarily small compared to the lower-order terms. Use of Eqs. (3.10) and (B1) then leads to the decomposition of J_m,

$$J_m=J_{m0}+\Delta J_m\,,$$

$$J_{m0}=\delta_{m1}f(1)\lambda(1)\,,\tag{B5}$$

$$\Delta J_2(1,2)=\Delta I_2(1,2)-f(1)\Delta I_1(2)\,,$$

and so on. Applying the scaling (3.13) and (3.15) to Eqs. (3.10) and (B5) thus leads to

$$J_{10}\to S^{-2}f(1)\lambda(1),\quad \Delta J_m\to S^{-3m}\Delta J_m\,.\tag{B6}$$

The first-order correction term ΔJ_1 in the kinetic equation (3.23) becomes important on the time scale of order T'. Since the free propagator g^0 is scaled as

$$g_{ij}^0(t)=\frac{T^{-3/2}\exp[-|\mathbf{r}_{ij}/l|^2/(4Dt/T)]}{(4\pi Dt/T)^{3/2}}\,.\tag{B7}$$

one can here make such a simple approximation in Eq. (B3) that all times t_i contained in the function F_n^m may be replaced by t,

(v)

(Λ)

FIG. 15. The diagrammatic expression of the renormalized perturbation expansions of $S^1\Delta J_1^s$ up to order S^0.

$$F_n^m(1,t;\ldots;m,t;m+1,t_{m+1};\ldots;n,t_n)$$

$$=F_n^m(1,t;\ldots;m,t;m+1,t;\ldots;n,t)$$

$$+O\left[(t-t_i)\left[\frac{\partial}{\partial t}\right]\right]\,,\tag{B8}$$

where $(t-t_i)(\partial/\partial t)$ is of order $T/T'=\Phi^{1/2}$. Then the errors introduced by this expansion have no effect on the first-order correction.

The F_n^m expression rapidly becomes unwieldy as n increases. In the following, therefore, it is convenient to use the same diagrammatic representations as those introduced by Tokuyama [29]. The diagram elements and their algebraic expressions are given in Table III. The diagrammatic representation of ΔJ_1^s is then given in Fig. 15. Its algebraic expression thus leads to Eq. (3.26).

APPENDIX C: DERIVATION OF EQS. (3.35) AND (4.5)

Similarly to Eq. (3.26), the scaled functions $S^d J_2^S$ and $S^{2d}J_3^S$ are expanded in powers of S^{-1} as in Fig. 16. The algebraic expression of $S^d J_2^S$ is then given by

$$S^d J_2^S(R_1,R_2,\mathbf{r}_1,\mathbf{r}_2;t)$$

$$=m_{22}(t,t)G_2(1,2;t)$$

$$-\int_0^t dt_3 R_2 g_{21}(t-t_3,t)\lambda(1;t_3)f(1;t)f(2;t)$$

$$+S^{-1}[\Delta X_{12}(t)+\Delta Y_{12}(t)]+O(S^{-2})\,.\tag{C1}$$

In the scaling limit $S\to\infty$, Eq. (3.25) thus reduces to Eq. (3.35).

Next we derive Eq. (4.5). The correction terms ΔX_{12} and ΔY_{12} of Eq. (C1) become important on the time scale of order T'. On such a time scale, therefore, the propagators g_{12}^0 and g_{12} in Fig. 16 are replaced by ξ_{12}^0 and ξ_{12}, respectively. The algebraic expressions of ΔX_{12} and ΔY_{12} are then given by

$$\Delta X_{12}(t) = \int d(3) v_{23}(f)\chi(3,1;t) - \delta(1-2)v(2)f(2) , \qquad (C2)$$

$$\Delta Y_{12}(t) = -\xi_{21} m_{12} G_2^\infty(1,2) + \int d(3) \left[\xi_{23}\xi_{31}\lambda(1)f(2)G_2^\infty(1,3) - \Lambda_{23}(f)\chi(3,1) - \delta(1-2)\int d(4)\xi_{23}\xi_{34}\lambda(4)f(2)G_2^\infty(3,4) \right.$$

$$\left. -\xi_{23} m_{32} \left\{ G_3^\infty(1,2,3) - \int d(4)[\delta G_2^\infty(2,3)/\delta f(4)]\chi(4,1) \right\} \right] , \qquad (C3)$$
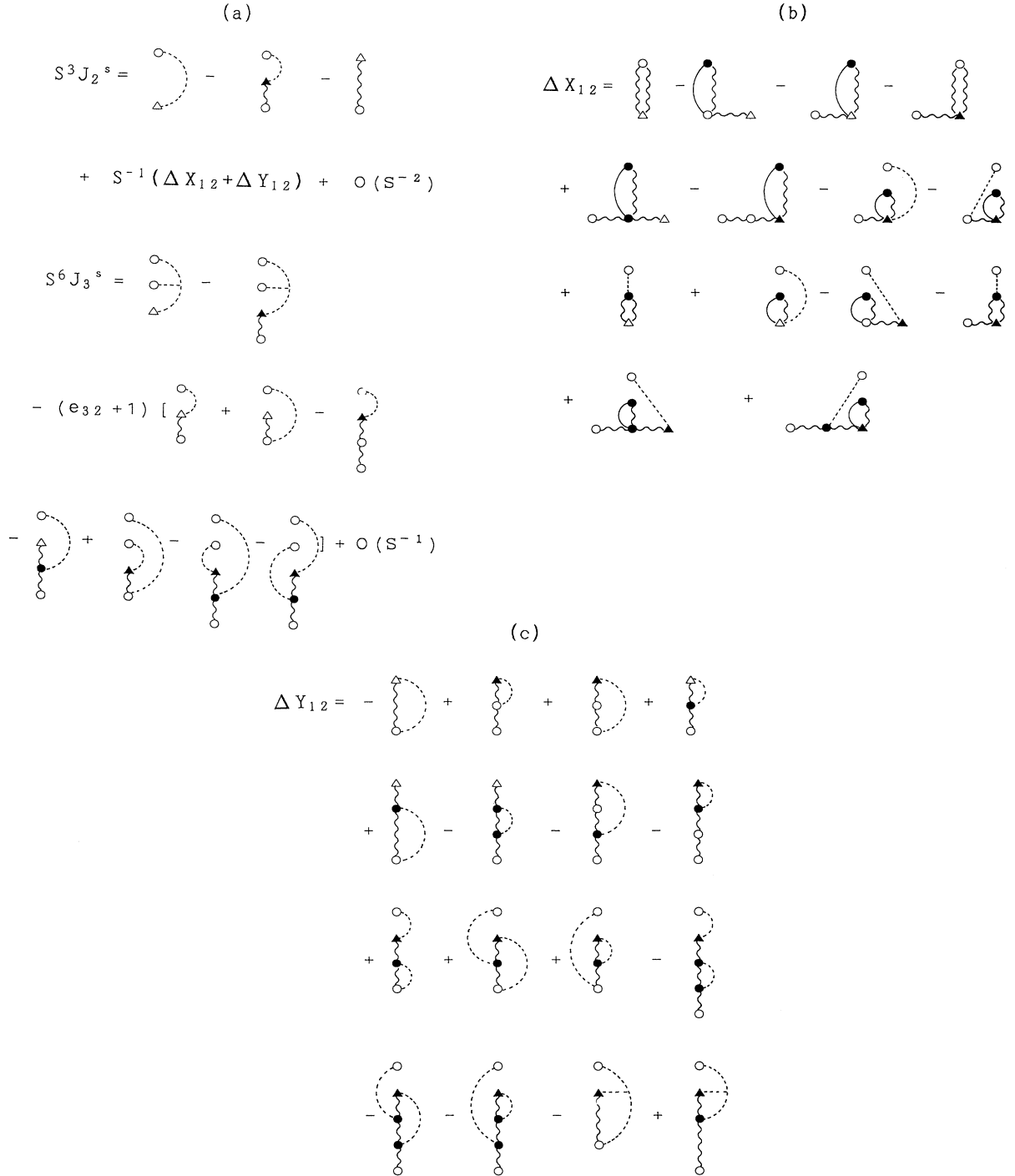

FIG. 16. (a) The diagrammatic expression of the renormalized perturbation expansions of $S^3 J_2^s$ and $S^6 J_3^s$ up to order S^{-1} and S^0, respectively. (b) The diagrammatic representation of ΔX_{12}. (c) The diagrammatic representation of ΔX_{12}. (c) The diagrammatic representation of ΔY_{12}.

where $v_{23}(f)=\delta[v(2)f(2)]/\delta f(3)$ and $\Lambda_{23}(f)=\delta[\Lambda(2)f(2)]/\delta f(3)$. Neglecting the spatial inhomogeneities of the distribution function $f(i)$ and applying the double-time scaling to Eq. (3.24) we thus obtain Eq. (4.5).

Finally we discuss the explicit form of the triple correlation function G_3^∞ which appears in Eq. (C3). In order to obtain G_3^∞, we further need to calculate J_3. From Fig. 16(a), the algebraic expression of $S^{2d}J_3^S$ is given by

$$S^{2d}J_3^S(R_1,R_2,R_3,\mathbf{r}_1,\mathbf{r}_2,\mathbf{r}_3;t)=m_{33}(t,t)G_3(1,2,3;t)-(1+e_{32})W(1,2,3;t)+O(S^{-1}) , \tag{C4}$$
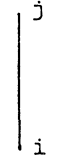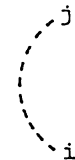
with

$$W(1,2,3;t)=\xi_{32}\lambda(2)[f(2)G_2(1,3)+f(3)G_2(1,2)]$$

$$-\int d(4)\left\{[\xi_{32}\xi_{24}\lambda(4)+\xi_{34}\xi_{42}\lambda(2)]f(2)f(3)G_2(1,4)\right.$$

$$\left.-\xi_{34}\lambda(4)G_2(1,3)G_2(2,4)+\int d(5)[\xi_{34}\xi_{45}\lambda(5)f(3)[G_2(2,4)G_2(1,5)+G_2(2,5)G_2(1,4)]]\right\} .$$

The scaling of Eq. (3.9) thus leads to $\qquad\qquad$ (C5)

TABLE III. The diagram elements used in the present paper.

Diagram elements	Algebraic expression	Order in S^{-1}
$\bigcirc\ i$	$f(i)$	S^{-2}
$\bullet\ i$	$\int d(i)f(i)$	S
$\triangle\ i\ =\ \bigcirc\ i\ -$	$\lambda(i;t_i)f(i)$	S^{-2}
$\blacktriangle\ i\ =\ \bullet\ i\ -$	$\int d(i)\lambda(i;t_i)f(i)$	S
	$\int dt_j g_{ij}^0(t_i-t_j)$	S^{-1}
	$\int dt_j g_{ij}(t_i-t_j)$	S^{-1}
	$G_2(i,j)$	S^{-5}

$$\left[\frac{\partial}{\partial t}\right]G_3(1,2,3;t)=-QD(1+e_{31}+e_{32})\left[\frac{\partial}{\partial R_3}\right]R_3^{-1}[m_{33}G_3(1,2,3;t)-W(1,2,3;t)] \ . \tag{C6}$$

This is then integrated to give the formal solution for large t,

$$G_3^\infty(1,2,3;t)=-\int_0^\infty ds \exp\left[-sQD(1+e_{31}+e_{32})\left[\frac{\partial}{\partial R_3}\right]R_3^{-1}m_{33}\right]QD(1+e_{31}+e_{32})\left[\frac{\partial}{\partial R_3}\right]R_3^{-1}W(1,2,3;t) \ ,$$

$$\tag{C7}$$

where we have neglected the initial triple correlation $G_3(t=0)$.

APPENDIX D: DERIVATION OF EQ. (3.56)

Using the Fourier-Laplace transformation, we can write Eq. (3.41) as

$$\Lambda(1)f(1)=(3\Phi/\mu_3)^{1/2}\int d\mathbf{x}_2\rho_1\xi(x_{12})$$

$$\times \int d\mathbf{q}\left[\exp(i\mathbf{q}\cdot\mathbf{x}_{12})B_q(\rho_1;\delta)-\rho_2 F(\rho_1)\int d\mathbf{x}_3\xi(x_{23})\int d\rho_3\lambda(3)\exp(i\mathbf{q}\cdot\mathbf{x}_{32})B_q(\rho_3;\delta)\right]\Big/(q^2+1) \ ,$$

$$\tag{D1}$$

with

$$B_q(\rho_1;\delta)=4\pi\int d\rho_2\lambda(2)[\delta+O_1+O_2-M_1(q)-M_2(q)]^{-1}(1+e_{12})O_1\rho_1\lambda(2)f(1)f(2) \ , \tag{D2}$$

where O_i and M_i are operators and given by

$$O_i=\left[\frac{\partial}{\partial\rho_i}\right]\rho_i^{-2} \ ,$$

$$M_i(q)=[O_i\rho_2 F(\rho_i)/(q^2+1)]\int d\rho_j\lambda(j)e_{ij} \ . \tag{D3}$$

By using the operator identity

$$[\delta+O_i-M_i]^{-1}=[\delta+O_i]^{-1}$$
$$+[\delta+O_i]^{-1}M_i[\delta+O_i-M_i]^{-1} \ , \tag{D4}$$

calculating each term of Eq. (D2) and summing over the resulting series, we thus find

$$B_q(\rho_1;\delta=0)=4\pi q^{-2}\left[-\lambda(1)+\frac{\langle\lambda^2\rangle}{\beta\mu_{-1}}O_1\rho_1\right]f(1) \ , \tag{D5}$$

where we have omitted the terms higher than the second-order derivatives in O_1. This is combined with Eq. (D1) to obtain Eq. (3.56).

APPENDIX E: DERIVATION OF EQS. (3.64), (3.65), AND (3.67)

We first derive Eqs. (3.65) and (3.67). Use of Eqs. (2.12) and (3.57) leads to

$$\left[\frac{d}{d\tau}\right]\Phi=-3Q\langle\lambda\rangle v/\tau_s \ . \tag{E1}$$

By using Eqs. (3.53) and (E1), we then obtain

$$\beta=\langle a\rangle\Delta(\tau)/Q \ . \tag{E2}$$

We expand the relative-droplet-size distribution function $F(\rho,\tau)$ in powers of τ to obtain

$$F(\rho,\tau)=F_0(\rho)+F_1(\rho)\tau^{-y_1}+F_2(\rho)\tau^{-y_2}+\cdots \ , \tag{E3}$$

where the terms are ordered so that $0<y_1<y_2\ldots$. In the following we discuss only the case where τ is close to τ_c. Since we have $\Phi\sim Q$ near τ_c, use of Eqs. (2.11), (2.12), and (E1) then leads to

$$\Delta(\tau)/Q=-\delta_1\tau^{-y_1}-\delta_2\tau^{-y_2}-\ldots \ , \tag{E4}$$

where δ_i is a constant to be determined. From Eqs. (3.51), (E2), and (E4), we then obtain

$$\langle\lambda\rangle(\tau)=1+\langle a\rangle[\delta_1\tau^{-y_1}+\delta_2\tau^{-y_2}+\cdots] \ . \tag{E5}$$

Since $\langle\lambda\rangle\sim 0$ near τ_c, from Eq. (E5), we thus find $\delta_1\tau^{-y_1}=-\langle a\rangle^{-1}$. This leads to $y_1=\eta_R$. To derive the values of the higher order y_n's, we write down the expansion for Eq. (E1) as

$$-y_1\delta_1\tau^{-y_1}-y_2\delta_2\tau^{-y_2}-\cdots$$
$$=-(3/\tau_s)v\tau\langle a\rangle[\delta_2\tau^{-y_2}+\delta_3\tau^{-y_3}+\cdots] \ . \tag{E6}$$

The time dependence of the left- and right-hand side of Eq. (E6) can only be balanced if all $y_n=n\eta_R$. Hence we find

$$\delta_n\tau^{-y_n}=-(y_1 y_2\cdots y_{n-1})(\tau_s/3v\tau)^{(n-1)}\langle a\rangle^{-n} \ . \tag{E7}$$

Use of Eqs. (E5) and (E6) then leads to

$$\langle\lambda\rangle=-y_1(\tau_s/3v\tau\langle a\rangle)[1+y_2(\tau_s/3v\tau\langle a\rangle)+\cdots] \ , \tag{E8}$$

where $y_n = n\eta_R$. Hence we obtain Eq. (3.65). We note here that the above derivation is also valid for stage $[C]$. Therefore, we also obtain Eq. (3.67).

We next derive Eq. (3.64). In stage $[I]$, from Eq. (3.71), we have the relation

$$v(\tau)\tau^{\eta_n} = v(\tau_s)\tau_s^{\eta_n} \ . \tag{E9}$$

In stage $[C]$, from Eq. (3.69), we have

$$v(\tau)\tau = v(\tau_c)\tau_c = \tau_s / (K_\infty \mu_3^\infty) \ . \tag{E10}$$

Assuming that Eq. (E9) holds even at $\tau = \tau_c$, and using Eq. (E10), we find

$$\tau_c = \tau_s (K_\infty \mu_3^\infty v_s)^{-1/(1-\eta_n)} \ . \tag{E11}$$

Since this holds even in the limit $Q \to 0$, we have

$$\tau_c / \tau_s \sim K_\infty (Q=0)^{-1/(1-\eta_n)} \ . \tag{E12}$$

Since $K_\infty \sim K(\tau_c)$, use of Eqs. (3.65) and (E12) then leads to $\langle a \rangle (\tau_c)^3 \sim (\tau_c / \tau_s)^{3(1-\eta_n)}$ in stage $[I]$. On the other hand, we have $\langle a \rangle (\tau_c)^3 \sim \tau_c$ in stage $[C]$. Therefore, we find $\eta_n = 2/3$ and obtain Eq. (3.64).

APPENDIX F: DERIVATION OF EQ. (4.15)

Use of Eqs. (3.11) and (4.14) leads to

$$(\underline{1} - \underline{P}) \cdot \underline{\chi}_k = (\underline{1} - \underline{P}) \cdot \underline{G}_k \ . \tag{F1}$$

Using $\underline{\chi}_k = \underline{P} \cdot \underline{\chi}_k + (\underline{1} - \underline{P}) \cdot \underline{\chi}_k$, we can write Eq. (4.13) as

$$\left[\frac{d}{d\tau} \right] S_k(\tau) = (2/\langle a \rangle^3) h(p,q) S_k(\tau)$$

$$+ 2\langle a \rangle^5 (4\pi/3)^2 \underline{u}_p \cdot \hat{\underline{O}} \cdot \underline{H}_q \cdot (\underline{1} - \underline{P}) \cdot \underline{G}_k \cdot \underline{u}_p$$

$$+ 2(4\pi/3)(3\Phi/\mu_3)^{3/2} B(p,q) \ . \tag{F2}$$

We next discuss the term $(\underline{1} - \underline{P}) \cdot \underline{G}_k$. By using Eqs. (3.11) and (4.5), one can generalize Eq. (3.35), to order $\Phi^{1/2}$, as

$$\left[\frac{\partial}{\partial \tau} \right] \underline{G}_k = (\underline{1} + \underline{e}) \cdot \hat{\underline{O}} \cdot [\underline{H}_k \cdot \underline{G}_k - \underline{T}_k] \ , \tag{F3}$$

where the source term $\underline{T}_k$ contains the term of order $\Phi^{1/2}$. This is formally solved to give

$$\underline{G}_k(\tau) = \int_0^\tau ds \, \exp[(\tau - s)\hat{\underline{O}} \cdot \underline{H}_k]$$

$$\times \{ \underline{G}_k(s)^* \cdot \underline{H}_k^* \cdot \hat{\underline{O}}^* - \underline{T}_k(s)^* \} \ , \tag{F4}$$

where $\underline{G}_k(0) = 0$. by using the operator identity

$$(\underline{1} - \underline{P}) \cdot \exp[t\hat{\underline{O}} \cdot \underline{H}_k] = \underline{V}_k(t)^* \cdot (\underline{1} - \underline{P}) + \int_0^t \underline{V}_k(s)^* \cdot (\underline{1} - \underline{P}) \cdot \hat{\underline{O}} \cdot \underline{H}_k \cdot \underline{P} \cdot \exp[(t-s)\hat{\underline{O}} \cdot \underline{H}_k] \ , \tag{F5}$$

and multiplying Eq. (F4) by $(\underline{1} - \underline{P})$, we obtain

$$(\underline{1} - \underline{P}) \cdot \underline{G}_k(\tau) = \int_0^\tau ds \, \underline{V}_k(s)^* \cdot (\underline{1} - \underline{P}) \cdot \hat{\underline{O}} \cdot \underline{H}_k \cdot \underline{P} \cdot \underline{G}_k(\tau - s) \ , \tag{F6}$$

where we have simply neglected the first term of Eq. (F5). Use of Eqs. (3.11), (F2), and (F6) then leads to Eq. (4.15).

*Permanent address: Department of Physics, Nagoya Institute of Technology, Nagoya 466, Japan.

[1] Y. C. Chou and W. I. Goldburg, Phys. Rev. A **23**, 858 (1981).

[2] M. Hennion, D. Ronzaud, and P. Guyot, Acta Metall. **30**, 599 (1982).

[3] S. Katano and M. Iizumi, Phys. Rev. Lett. **52**, 835 (1984).

[4] C. M. Knobler and N. C. Wong, J. Phys. Chem. **85**, 1972 (1981).

[5] K. Osamura, H. Okuda, and S. Ochiai, Scr. Metall. **19**, 1379 (1985); K. Osamura, H. Okuda, Y. Amemiya, and H. Hashizume, Metall. Trans. **19A**, 1973 (1988).

[6] M. Furusaka, Y. Ishikawa, and M. Mera, Phys. Rev. Lett. **54**, 2611 (1985).

[7] A. Cumming, P. Wiltzius, and F. S. Bates, Phys. Rev. Lett. **65**, 863 (1990); A. Cumming, P. Wiltzius, F. S. Bates, and J. H. Rosendale, Phys. Rev. A **45**, 885 (1992).

[8] J. Marro, J. L. Lebowitz, and M. H. Kalos, Phys. Rev. Lett. **43**, 282 (1979).

[9] J. L. Lebowitz, J. Marro, and M. H. Kalos, Acta Metall.

30, 297 (1982).

[10] P. Fratzl, J. L. Lebowtiz, J. Marro, and M. H. Kalos, Acta Metall. **31**, 1849 (1983).

[11] K. Binder and D. Stauffer, Phys. Rev. Lett. **33**, 1006 (1974).

[12] K. Binder, Phys. Rev. B **15**, 4425 (1977).

[13] H. Furukawa, Prog. Theor. Phys. **59**, 1072 (1978); Phys. Rev. Lett. **43**, 136 (1979).

[14] J. S. Langer and A. J. Schwartz, Phys. Rev. A **21**, 948 (1980.

[15] *Nucleation*, edited by A. C. Zettlemoyer (Dekker, New York, 1969).

[16] K. Binder and D. Stauffer, Adv. Phys **25**, 343 (1976).

[17] I. M. Lifshitz and V. V. Slyozov, J. Phys. Chem. Solids **19**, 35 (1961).

[18] C. Wagner, Z. Electrochem. **65**, 581 (1961).

[19] M. Tokuyama and K. Kawasaki, Physica A **123**, 386 (1984); M. Tokuyama, K. Kawasaki, and Y. Enomoto, *ibid.* A **134**, 323 (1986); M. Tokuyama, Y. Enomoto, and K. Kawasaki, *ibid.* A **143**, 183 (1987).

[20] J. A. Marqusee and J. Ross, J. Chem. Phys. **79**, 373 (1983); **80**, 536 (1984).

[21] P. W. Voorhees and M. E. Glicksman, Acta Metall. **32**, 2001 (1984); **32**, 2013 (1984).

[22] J. D. Gunton, M. San Miguel, and P. S. Sahni, in *Phase Transitions and Critical Phenomena*, edited by C. Domb and J. L. Lebowtiz (Academic, New York, 1983), Vol. 8.

[23] K. Oki, H. Sagane, and T. Eguchi, J. Phys. C **7**, 414 (1977).

[24] W. C. Johnson, Acta Metall. **32**, 465 (1984).

[25] C. Yeung, Phys. Rev. Lett. **61**, 1135 (1988).

[26] H. Furukawa, J. Phys. Soc. Jpn. **58**, 216 (1989); Phys. Rev. B **40**, 2341 (1989).

[27] Y. Oono and S. Puri, Phys. Rev. A **38**, 434 (1988).

[28] P. Fratzl, J. L. Lebowtiz, O. Penrose, and J. Amar, Phys. Rev. B **44**, 4794 (1991).

[29] M. Tokuyama, Physica A **169**, 147 (1990).

[30] J. J. Wein and J. W. Cahn, Mater. Res. **6**, 151 (1973).

[31] K. Kawasaki and T. Ohta, Physica A **118**, 175 (1983).

[32] M. Tokuyama, in *Dynamics of Ordering Processes in Condensed Matter*, edited by S. Komura and H. Furukawa (Plenum, New York, 1988).

[33] For reviews, see *Dynamics of Ordering Processes in Condensed Matter*, edited by S. Komura and H. Furukawa (Plenum, New York, 1988).

[34] H. Mori, Prog. Theor. Phys. **53**, 1617 (1975); M. Tokuyama and H. Mori, *ibid.* **56**, 1073 (1976).

[35] F. S. Bates and P. Wiltzius, J. Chem. Phys. **91**, 3258 (1989).

[36] T. Ohta and H. Nozaki, in *Space-Time Organization in Macromolecular Fluids*, edited by F. Tanaka *et al.* (Springer, Berlin, 1989).

[37] A. Chakrabarti, R. Toral, J. D. Gunton, and M. Muthukumar, J. Chem. Phys. **92**, 6899 (1990).

[38] Y. Enomoto, K. Kawasaki, and M. Tokuyama, Acta Metall. **35**, 915 (1987).